Insights into the Role of the Metal-Binding Sites of Quercetin 2,3-Dioxygenase from *Bacillus subtilis*

by

Sara Bowen

A Dissertation Presented in Partial Fulfillment
of the Requirements for the Degree
Doctor of Philosophy

Approved October 2010 by the
Graduate Supervisory Committee:

Wilson Francisco, Chair
James Allen
Anne Jones

ARIZONA STATE UNIVERSITY
December 2010

ABSTRACT

The metalloenzyme quercetin 2,3-dioxygenase (QueD) catalyzes the oxidative decomposition of the aromatic compound, quercetin. The most recently characterized example is a product of the bacterium *Bacillus subtilis* (BsQueD); all previous examples were fungal enzymes from the genus *Aspergillus* (AQueD). AQueD contains a single atom of Cu(II) per monomer. However, BsQueD, over expressed in *Escherichia coli*, contains Mn(II) and has two metal-binding sites, and therefore two possible active sites per monomer. To understand the contribution of each site to BsQueD's activity, the N-terminal and C-terminal metal-binding sites have been mutated individually in an effort to disrupt metal binding. In wild type BsQueD, each Mn(II) is ligated by three histidines (His) and one glutamate (Glu). All efforts to mutate His residues to non-ligating residues resulted in insoluble protein or completely inactive enzyme. A soluble mutant was expressed that replaced the Glu residue with a fourth His at the N-terminal domain. This mutant (E69H) has a specific activity of 0.00572 μmol/min/mg, which is nearly 3000-fold lower than the rate of wild type BsQueD (15.9 μmol/min/mg). Further analysis of E69H by inductively couple plasma mass spectrometry revealed that this mutant contains only 0.062 mol of Mn(II) per mol of enzyme. This is evidence that disabling metal-ligation at one domain influences metal-incorporation at the other.

During the course of the mutagenic study, a second, faster purification method was developed. A hexahistidine tag and an enterokinase cleavage site were fused to the N-terminus of BsQueD (6xHis-BsQueD). Active enzyme was successfully expressed and purified with a nickel column in 3 hours. This is much faster than the previous multi-column purification, which took two full days to complete. However, the concentration of soluble, purified enzyme (1.8 mg/mL) was much lower than concentrations achieved with the traditional method (30 mg/mL). While the concentration of 6xHis-BsQueD is sufficient for some analyses, there are several characterization techniques that must be conducted at higher concentrations. Therefore, it will be advantageous to continue using both purification methods in the future.

DEDICATION

I dedicate this dissertation to my mom because she kept reminding me that it would get written. I dedicate it to Jay because he has listened patiently to every word I've written in it. I also dedicate it to Tracy, Sherri, Becki, Wei-Jen and Jenn because they have been a constant support system. And finally I dedicate it to Ross, Laura and Dad. Listen, I'm only gonna 'splain this once. Got it?

ACKNOWLEDGMENTS

I would like to acknowledge my advisor, Dr. Wilson Francisco for all his patience and advice. I would also like to acknowledge all the students who have been in the lab-especially Dr. Matthew Schaab, Qin Yan, Matt Simon, James Cronican, Kevin Smith, and Sonya Becker. And thank you to my committee members, Dr. James Allen and Dr. Anne Jones. I relied heavily on your expertise in the last two years of graduate school, and I appreciate all your valuable advice. I would also like to thank Dr. Rebekka Wachter for her questions and suggestions about my project while I've been in graduate school. Finally I would like to thank Dr. Petra Fromme for stopping by my poster every semester even though she is not on my dissertation committee.

TABLE OF CONTENTS

Page

LIST OF TABLES

LIST OF FIGURES

Figure Page

Figure Page

Figure Page

Figure Page

Chapter 1

AN INTRODUCTION TO QUERCETIN 2,3-DIOXYGENASE

INTRODUCTION

Enzymes are generally substrate-specific and can only perform catalysis on a small range of molecules because enzyme structure directly influences enzyme function. For example, enzymes must be geometrically and electronically complimentary to their substrates to undergo catalysis. This means that a substrate must physically fit into the active site cavity, and enzyme residues within the cavity must interact with the substrate to hold it in place until the reaction is complete. Therefore understanding the specific spatial interactions between substrate and enzyme is crucial to understanding the process of catalysis (1).

This study was designed to learn how the enzyme, quercetin 2,3-dioxygenase, oxidatively cleaves the cyclic, organic molecule, quercetin. Several techniques were combined to learn what the active site environment is like before and during the enzymatic reaction. With this information it will be possible to alter the enzyme to metabolize a range of organic compounds, which will be useful for disposing of harmful organic molecules.

Cupin Proteins. Cupin proteins are characterized by a conserved beta-barrel fold; the name is in fact derived from the Latin word for barrel, ‘cupa’. First identified in the plant protection proteins germin and germin-like proteins (GLPs),

the classification now encompasses at minimum 18 different functional classes including but not limited to: isomerases, epimerases, oxygenases, and decarboxylases- making it the most functionally diverse protein superfamily known to date. This particular fold results from the following loosely-conserved, 2-motif amino acid sequence: $G(X)_5\underline{H}X\underline{H}(X)_{3,4}\underline{E}(X)_6G$ and $G(X)_5PXG(X)_2\underline{H}(X)_3N$ (2). The semi-conservative nature of the cupin motifs allows for the vast functional diversity of the cupin superfamily members. Additionally, the amino acids underlined in the above sequence have been shown to bind several metal ions. The majority of cupins bind iron, but there are examples of cupin proteins that contain copper, zinc, cobalt, nickel and manganese. The ability to bind different metal cofactors further increases the range of possible functions of cupin proteins (3). For example, one protein in the methionine salvage pathway of *Klebsiella pneumoniae* has been shown to function as two different dioxygenases simply by changing the identity of the metal cofactor (4,5).

This superfamily can be broadly divided into two groups, monocupins versus bicupins. The bicupins, a subclass of the cupin superfamily, contain the structural cupin fold twice within a single domain. This is likely the result of a gene duplication event during the evolution of bicupin proteins. Although in a few examples it is possible that two different monocupins fused to form a bicupin descendent (3,6).

Dioxygenases. The atmosphere consists of ~20% oxygen, which exists in two spin states, singlet and triplet (7-9). Because it readily reacts with organic molecules, the singlet state of oxygen is rarely observed. Therefore, an organic substrate will not often react with atmospheric oxygen, and it must first become activated (or interact with activated oxygen) to react. This is often accomplished by catalysis with enzymes containing metals or organic cofactors (10).

Oxygenases, which constitute the largest portion of the cupin superfamily but are not confined to it (2), are one type of enzyme capable of activating oxygen by incorporating one (in the case of mono-oxygenases) or both (in the case of dioxygenases) of the atoms of molecular oxygen into the catalytic product. Among catecholic compounds, there are two major categories of dioxygenases: intradiol and extradiol. Each type of enzyme cleaves a carbon-carbon bond in the process of oxidation, but as the name implies, intradiol dioxygenases cleave the bond between each hydroxyl group while the extradiol dioxygenases break a carbon-carbon bond outside and adjacent to the hydroxyl groups (FIG. 1.1). Both types of dioxygenases utilize iron for catalytic activity, which is seen in the vast majority of dioxygenases, but interestingly, the intradiol dioxygenases tend to use ferric iron while the extradiol enzymes contain ferrous iron, and most lose function when forced to bind the opposite iron species (8).

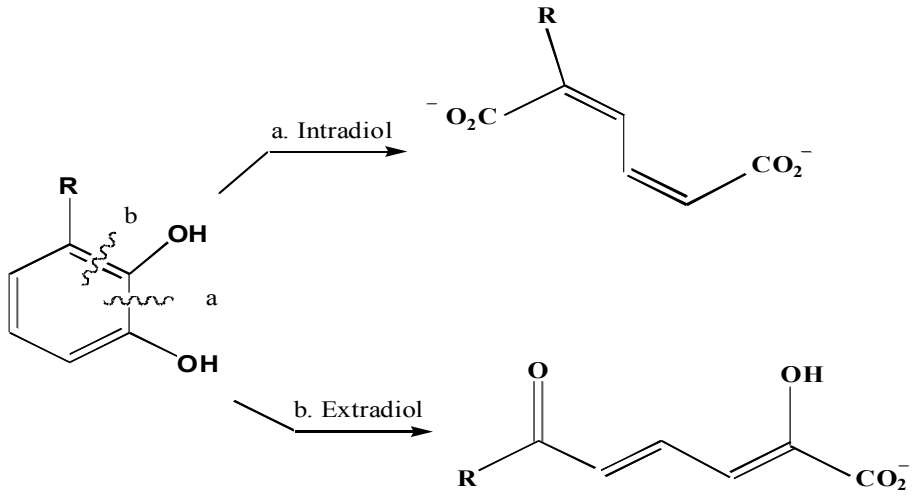

FIG. 1.1: **Extradiol and Intradiol Cleavage.** Extradiol and intradiol dioxygenases cleave carbon-carbon bonds at different positions on catechol molecules during oxidation. In most examples of catechol dioxygenases, intradiols utilize ferric iron exclusively while the extradiols are restricted to ferrous iron (8).

*Quercetin 2,3 Dioxygenase***.** Quercetin 2,3-dioxygenase (QueD) catalyzes the oxidative cleavage of the three-ringed substrate, quercetin, to produce 2-protocatechuoylphloroglucinol carboxylic acid and carbon monoxide (FIG. 1.2). The reaction is unusual because only a handful of proteins are known to produce carbon monoxide. In the late 1960s and early 70s, QueD was first purified from the secretions of the filamentous fungus, *Aspergillus flavus* (AfQueD). It was found that under non-ideal conditions, *A. flavus* could live with quercetin or its precursor rutin as its only carbon source, and that a single enzyme, AfQueD, was

capable of degrading quercetin in this metabolic pathway (11). This enzyme is unique in that it is the only dioxygenase known to contain a copper ion in its active site (12,13). AfQueD and its gene have yet to be completely sequenced, but a similar QueD from the same genus, *Aspergillus japonicus* (AjQueD), has been sequenced. In 2002, the structure of AjQueD was solved by X-ray crystallography to 1.6≈ resolution (14). This experiment determined that the type II copper ion is ligated by three histidines (His66, His68, and His112). A fourth ligand is sometimes a water molecule, but it was learned that sometimes the copper was ligated by a glutamate residue at position 73, which was confirmed by electron paramagnetic resonance (EPR). This is the first example of a natural enzyme with a carboxylate-ligated copper. Further modeling of the active site with quercetin revealed that not only does Glu73 act as a metal ligand, it may be functioning as a base, extracting a proton during catalysis from the 3'-OH of quercetin (12-14).

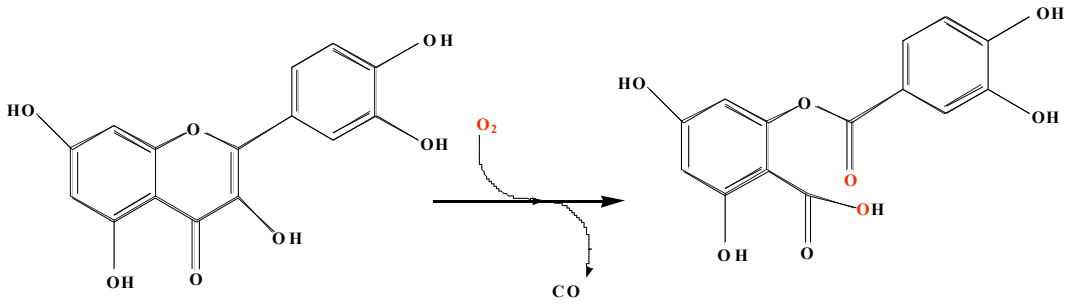

FIG. 1.2: **QueD catalytic reaction**. QueD cleaves two carbon-carbon bonds of the flavonol quercetin. During the reaction both atoms of molecular oxygen are incorporated into the product, 2-protocatechuoylphloroglucinol carboxylic acid, as can be seen by the red oxygen atoms. The reaction is fairly unique in that each molecule of quercetin produces one molecule of carbon monoxide.

A BLAST search was conducted with AjQueD, and one gene from the soil bacterium *Bacillus subtilis* was found which is 17% identical and 39% similar. This gene was over expressed in *E. coli* and the gene product was confirmed to be the first example of QueD activity from a prokaryotic protein although the initial analysis revealed a much less active enzyme when compared to the previously purified QueD from fungal organisms (15, 16).

Comparison of Aspergillus QueD to Bacillus QueD. When first over expressed and characterized, BsQueD was shown to contain 0.8 moles of iron per mole of enzyme, and its catalytic activity was nearly 100-fold lower than that of AfQueD (TABLE 1.1). Also the 3His1Glu metal-ligation was unusual among

iron-containing dioxygenases. The majority of other examples have been shown to utilize only 2His1Glu (17, 18 (FIG. 1.3)). This iron incorporation is likely a result of over expressing the protein in *E. coli* grown on the common rich media, Lurai Burtani (LB (19)). Experiments were conducted to improve the incorporation of other metal ions, such as Zn^{2+}, Cu^{2+}, Mn^{2+}, Mg^{2+}, Ni^{2+}, Cd^{2+} and Co^{2+}, into the active site. One method involved unfolding BsQueD in the presence of chaotrophic agents such as urea or guanidine chloride, dialyzing against chelating agents, then refolding the protein in the presence of a desired metal (20). An *in vivo* method was also very successful for several metals. In this method, the host bacterium was grown on M9 minimal media instead of LB. At the induction stage, an excessive amount of a particular metal was added. Previous experiments with *E. coli* have shown that available metal concentration is often an indicator of metal incorporation. Two metals, Mn^{2+} and Co^{2+}, were comparably or more highly incorporated and produced a more active enzyme than iron ((17) FIG. 1.4). Unfortunately, even very low concentrations of copper ions precipitate out of solution in M9 media. Therefore a different means of incorporating copper by denaturation/renaturation should be investigate. The high activity of Mn^{2+} in BsQueD is interesting because all other known QueDs had been shown to contain a type II Cu^{2+} center.

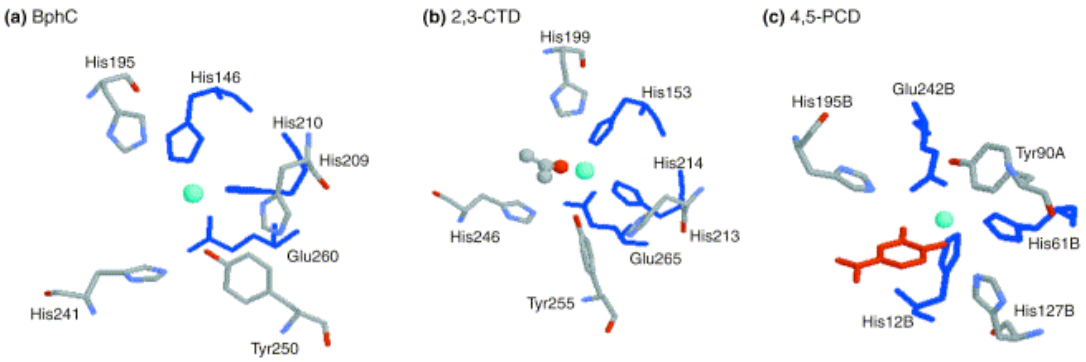

FIG 1.3: **Active sites of non-heme, iron dioxygenases**. The active sites of 3 non-heme, iron-containing dioxygenases have a 2His1Glu binding motif, which differs from the Fe^{2+}-coordination of BsQueD (FIG. 1.7). Metal-coordinated side chains are shown in bright blue, iron is shown as aqua. a) 2.3-dihydroxybiphenyl 1,2-dioxygenase from *Pseudomonas sp.* b) catechol 2,3-dioxygenase from *Pseudomonas putida* c) protocatechuate 4,5-dioxygenase from *Sphingomonas paucimobilis* (7).

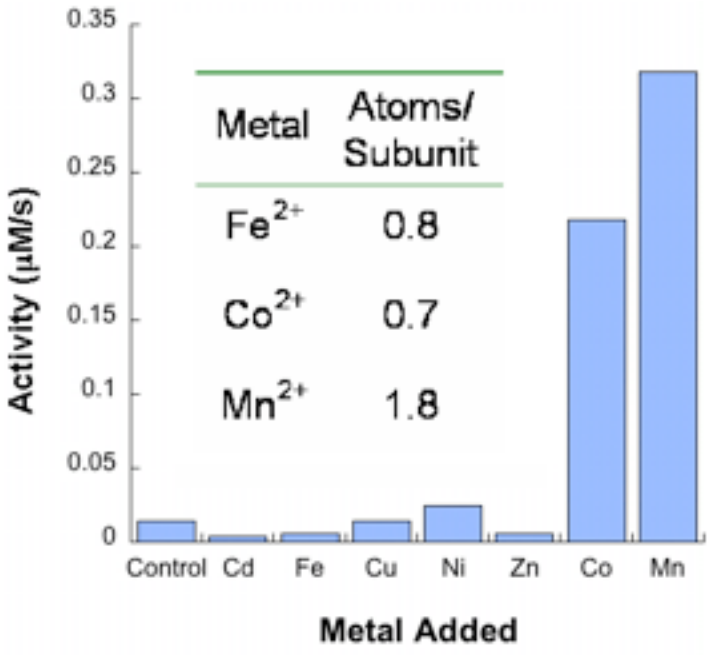

FIG. 1.4: **Metal incorporation and BsQueD activity**. Incorporation was accomplished by an *in vivo* technique, in which cells were grown on minimal media and supplemented with a given ion upon induction (21).

The crystal structure of BsQueD has been solved recently with Fe^{2+} in the active site. Comparisons of the N- and C-terminal metal-binding spheres of BsQueD to the N-terminal metal-binding site of AjQueD revealed very similar environments, which differ from the standard non-heme iron-containing dioxygenases ((20) FIG. 1.3).

One very obvious difference between AQueD and BsQueD is the number of metal-binding sites. Although AQueD is a bicupin enzyme because it has two regions of beta-barrel structure, only the N-terminal domain has the 3His, 1Glu

residues necessary for metal binding, while BsQueD is capable of binding metal at both the N-terminal and the C-terminal cupin domains. And inductively-coupled mass spectrometry (ICP-MS) experiments have shown that in the case of Mn^{2+}, BsQueD does in fact bind approximately 2 Mn^{2+} ions per monomer. Therefore, to understand the mechanism of action of BsQueD, it is essential to understand the contributions of each of these metal-binding sites to the enzymatic activity of BsQueD. To learn this, site-directed mutagenesis experiments have been designed and will be discussed in the following chapters (FIG. 1.5 and 1.6).

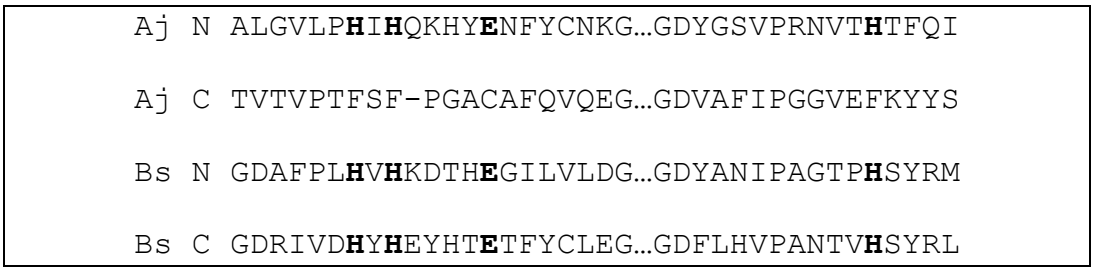

FIG. 1.5: **Sequence alignment of AQueD and BsQueD**. The cupin domains of QueD from *Aspergillus japonicus* and *from Bacillus subtilis* are very similar, but while the three histidines and single glutamate responsible for metal-binding are present in both cupin domains of the prokaryote example of QueD, the c-terminal domain metal-binding residues are absent in the fungal QueD.

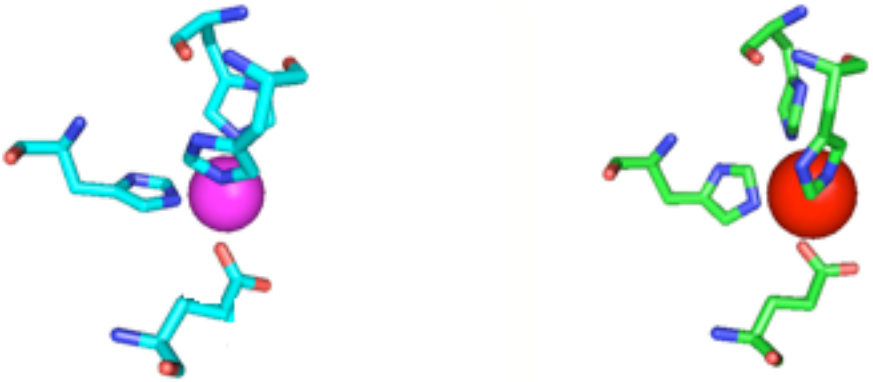

FIG. 1.6: **Active sites of AQueD and BsQueD**. Metal binding residues of AjQueD (left; ligating copper) and BsQueD (right; ligating iron) (14, 20).

The recently solved crystal structure of BsQueD also revealed the active site cavity of BsQueD is much more open than that of AjQueD because several of AjQueD's bulky residues (Tyr35, Met51, Thr53, Phe75, Phe114, Met123, and Ile127) have been replaced with smaller ones in BsQueD (Ala, Val, Leu, Ile, Tyr, Leu and Thr (20)). Understanding how this wider cavity affects catalysis will be much clearer once the enzyme:substrate complex structure has been solved (FIG. 1.7).

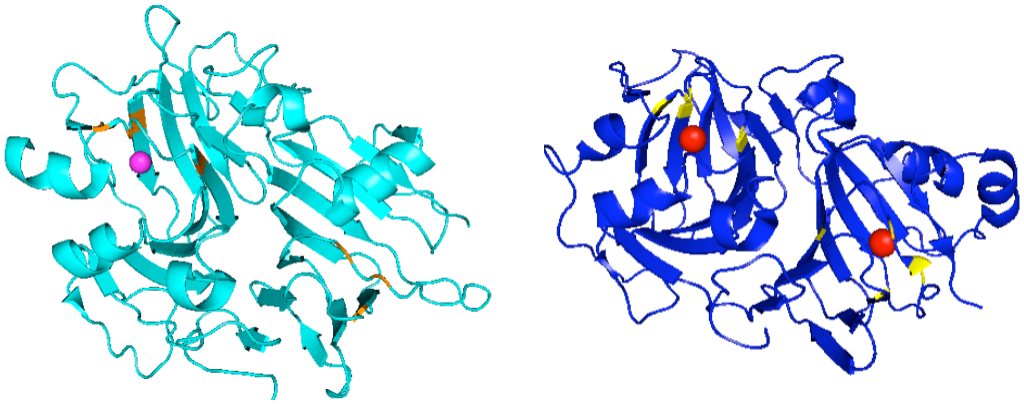

FIG. 1.7: **Crystal structure comparison of AQueD and BsQueD**. Crystal structure of AjQueD PBD 1juh (in cyan) versus the crystal structure of BsQueD PBD 1y3t (blue (14, 20)). In each structure, 2 beta-barrel folds can be seen, but in AjQueD only one domain contains a metal ion. Copper ions are shown in magenta; iron ions are shown in red. Some residues of the cupin domain are colored orange and yellow for AjQueD and BsQueD respectively. These residues are metal-binding (HHEH) in both domains of BsQueD and the N-terminal domain of AjQueD, but they are non-metal-binding (FFNF) in AjQueD's C-terminal domain.

Mechanisms have been proposed for both the fungal and the bacterial quercetinases. For both reactions the first step is deprotonation of the 3' hydroxyl group of quercetin by a nearby glutamate residue allowing quercetin to

bind to the metal through its 3' oxygen (FIG. 1.8). AjQueD shuttles a single electron from quercetin to the Cu^{2+} cofactor, thus activating the substrate for attack by singlet oxygen (FIG. 1.9). By contrast, BsQueD is proposed to activate the oxygen for reaction with the substrate by binding molecular oxygen through the Mn^{2+} cofactor, which can then act as an electron conduit (FIG. 1.10). In AjQueD, binding the oxygen directly is not likely because Cu^{2+} is already in the oxidized form. After activation, both reactions form an oxygen bridge from the metal to the 2C. It is possible that both reactions could follow the same degradation mechanism from this bridge point. One possibility is the addition of a hydrogen ion, which allows for Criegee rearrangement, which could then form the final product, protocatechuoyphloroglucinol carboxylic acid (FIG. 1.11 (17, 12)).

TABLE 1.1.

Summary of the differences between AQueD and BsQueD.

Organism	Number of Metal-Binding Sites	Identity of the Metal Cofactor	Method of Oxygen Activation	Relative Cavity Size
Aspergillus flavus (AfQueD) Aspergillus japonicus (AjQueD)	1	Cu^{2+}	The substrate is activated and interacts directly with O_2	Narrower
Bacillus subtilis (BsQueD)	2	Mn^{2+} (Fe^{2+})	O_2 is activated and can interact with the substrate.	Wider

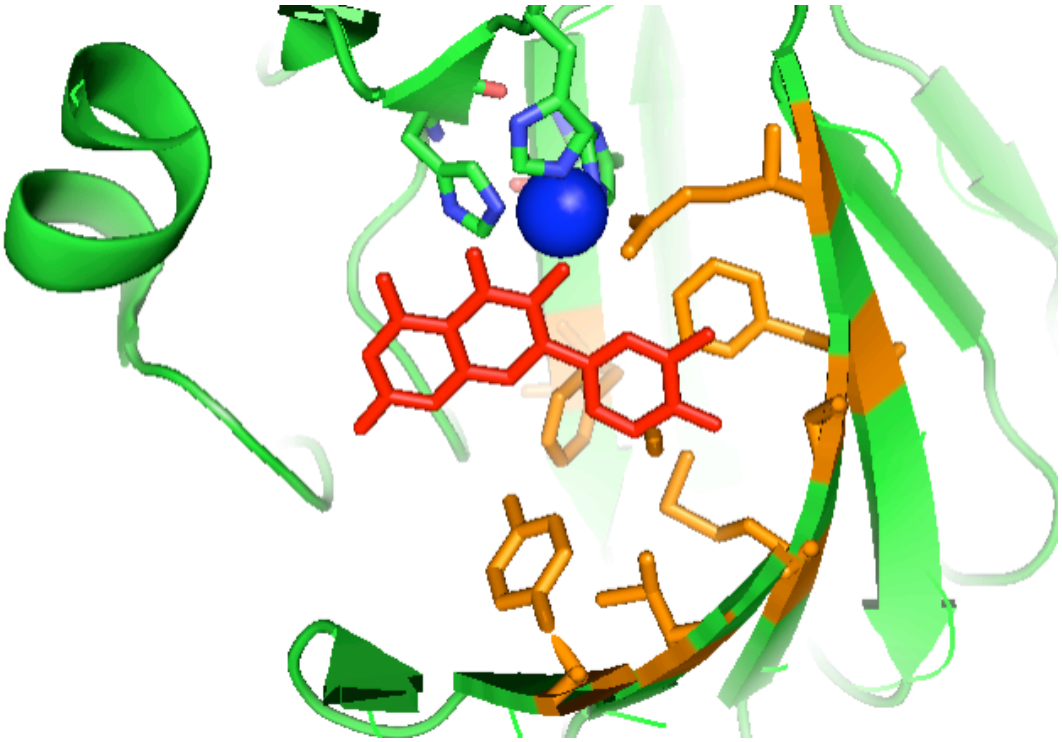

FIG. 1.8: **Active site of AQueD with bound substrate**. The active site of AjQueD crystallized anaerobically with its substrate, quercetin PBD 1h1i, directly before catalysis. Residues colored orange are likely involved in the stabilization of quercetin once in the active site. Metal binding residues are shown as sticks in green. The arrangement of the barrel forces quercetin to enter the cavity in this single orientation, exposing its 3' hydroxyl group to Glu73 (shown behind the metal ion) for deprotonation.

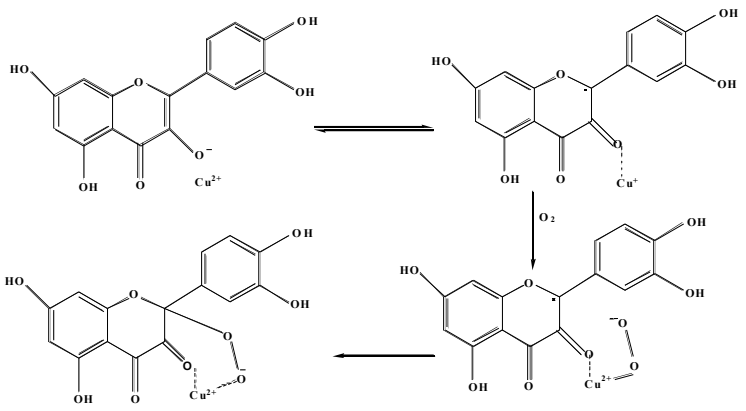

FIG. 1.9: **Substrate activation of AQueD**. The proposed activation of quercetin to react with oxygen in the enzyme AjQueD. In contrast to BsQueD (FIG. 1.10), AjQueD creates a quercetin radical before any interaction with oxygen, but an oxygen bridge intermediate, like that proposed in BsQueD, is formed allowing the decomposition to products to occur in the same or similar manner for both reactions (FIG. 1.11).

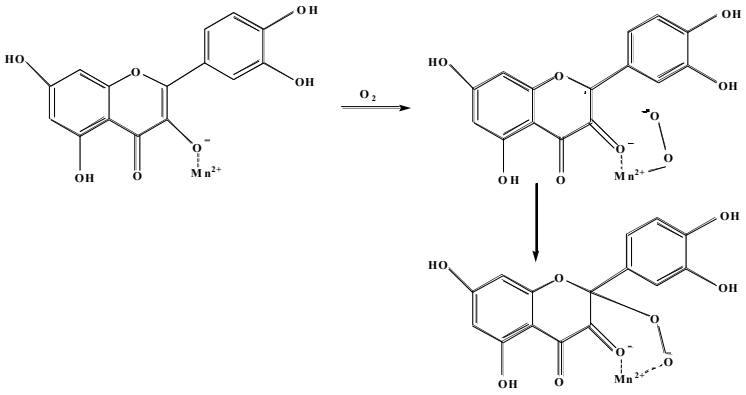

FIG. 1.10: **Oxygen activation of BsQueD**. The proposed activation of oxygen to react with quercetin in the enzyme BsQueD. Notice the metal binds both substrate and oxygen before creating the free radical that causes the oxygen bridge intermediate.

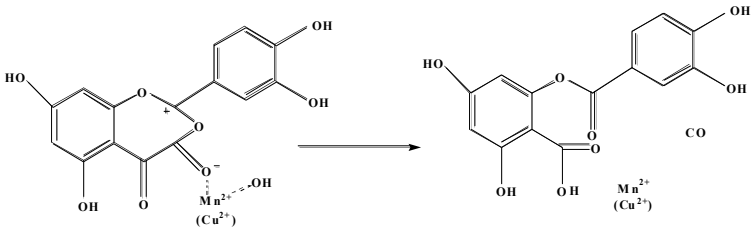

FIG. 1.11: **Decomposition of products**. The possible final steps of product formation for both reactions after the oxygen bridge intermediate. From the intermediate in figures 1.9 and 1.10, a Criegee rearrangement could form the intermediate shown above. The final product, protocatecuoyphloroglucinol carboxylic acid could form via an alkyl migration.

Project Goals. Although a mechanism has been proposed for the enzymatic reaction of BsQueD, it has yet to be modeled with a known BsQueD active site structure. (The only structure proposed contained inefficient iron ions in the active sites.) My research has been designed to achieve this by discovering the spatial orientation of active site residues and the identity of the most efficient catalytic metal cofactor. My main aim is to learn the individual contributions of the two metal-binding domains to catalytic activity. Additionally, I plan to continue exploring the mechanism of BsQueD by studying inhibition of catalysis.

*Metal-binding site contributions to catalysis***.** The bicupin, BsQueD, contains residues capable of binding metal in both its cupin domains. Therefore, it is possible that both domains contribute to the overall oxidation of quercetin. To better understand each domain's contribution to activity, site-directed mutagenesis experiments have been designed to disrupt metal binding in either the N-terminal or C-terminal cupin domains. Activity and structural studies can then be conducted on both mutants and compared to the wildtype.

Enzyme kinetics studies. To better understand the catalytic mechanism of BsQueD, an inhibitor, 3,7,3'-trihydroxyflavone, has been identified. Its inhibition has been analyzed as a function of pH to provide insight into the protonation states of the enzyme and the substrate.

REFERENCES

1. Voet, D., Voet, J. G., and Pratt, C. W. (2002) *Fundamentals of Biochemistry Upgrade Ed.* John Wiley & Sons, Inc, United States of America

2. Dunwell, J. M., Purvis, A., and Khuri, S. (2004) Cupins: the most functionally diverse protein superfamily? *Phytochemistry 65*, 7-17.

3. Dunwell, J. M., Culham, A., Carter, C. E., Sosa-Aguirre, C. R., and Goodenough, P. W. (2001) Evolution of functional diversity in the cupin superfamily. *Trends in Biochemical Sciences 26*, 740-746.

4. Dai, Y., Pochapsky, T. C., and Abeles, R. H. (2001) Mechanistic studies of two dioxygenases in the methionine salvage pathway of *Klebsiella pneumoniae*. *Biochemistry 40*, 6379-6387.

5. Dai, Y., Wensink, P. C., and Abeles, R. H. (1999) One protein, two enzymes. *Journal of Biological Chemistry 274*, 1193-1195.

6. Hawkins, A. R., and Lamb, H. K. (1995) The molecular biology of multidomain proteins - selected examples. *European Journal of Biochemistry 232*, 7-18.

7. Bugg, T. D. H. (2001) Oxygenases: mechanisms and structural motifs for O-2 activation. *Current Opinion in Chemical Biology 5*, 550-555.

8. Bugg, T. D. H. (2003) Dioxygenase enzymes: catalytic mechanisms and chemical models. *Tetrahedron 59*, 7075-7101.

9. Klinman, J. P. (2001) Life as aerobes: are there simple rules for activation of dioxygen by enzymes? *Journal of Biological Inorganic Chemistry 6*, 1-13.

10. Klinman, J. P. (2007) How Do Enzymes Activate Oxygen without Inactivating Themselves? *Accounts of Chemical Research* 40, 325-333.

11. Oka, T., Simpson, F. J., Child, J. J., and Mills, C. (1971) Degradation of rutin by *Aspergillus flavus* - Purification of dioxygenase, quercetinase. *Canadian Journal of Microbiology 17*, 111-&.

12. Steiner, R. A., Kalk, K. H., and Dijkstra, B. W. (2002) Anaerobic enzyme-substrate structures provide insight into the reaction mechanism of the copper-dependent quercetin 2,3-dioxygenase. *Proceedings of the National Academy of Sciences of the United States of America 99*, 16625-16630.

13. Steiner, R. A., Kooter, I. M., and Dijkstra, B. W. (2002) Functional analysis of the copper-dependent quercetin 2,3-dioxygenase. 1. Ligand-induced coordination changes probed by X-ray crystallography: Inhibition, ordering effect, and mechanistic insights. *Biochemistry 41*, 7955-7962.

14. Fusetti, F., Schroter, K. H., Steiner, R. A., van Noort, P. I., Pijning, T., Rozeboom, H. J., Kalk, K. H., Egmond, M. R., and Dijkstra, B. W. (2002) Crystal structure of the copper-containing quercetin 2,3-dioxygenase from *Aspergillus japonicus*. *Structure 10*, 259-268.

15. Barney, B. M., Schaab, M. R., LoBrutto, R., and Francisco, W. A. (2004) Evidence for a new metal in a known active site: purification and characterization of an iron-containing quercetin 2,3-dioxygenase from *Bacillus subtilis*. *Protein Expression and Purification 35*, 131-141.

16. Bowater, L., Fairhurst, S. A., Just, V. J., and Bornemann, S. (2004) *Bacillus subtilis* YxaG is a novel Fe-containing quercetin 2,3-dioxygenase. *Febs Letters 557*, 45-48.

17. Schaab, M. R., Barney, B. M., and Francisco, W. A. (2006) Kinetic and spectroscopic studies on the quercetin 2,3-dioxygenase from Bacillus subtilis. *Biochemistry 45*, 1009-1016.

18. Nidetzky, G. D. S. a. B. (2006) Variations of the 2-His-1-carboxylate Theme in Mononuclear non-Heme FeII Oxygenases. *ChemBioChem 7*, 1536-1548.

19. Gabbianelli, R., Battistoni, A., Polizio, F., Carri, M. T., Demartino, A., Meier, B., Desideri, A., and Rotilio, G. (1995) Metal uptake of

recombinant cambialistic superoxide dismutase from *Propionibacterium shermanii* affected by growth conditions of host *Escherichia coli* cells. *Biochemical and Biophysical Research Communications 216*, 841-847.

20. Gopal, B., Madan, L. L., Betz, S. F., and Kossiakoff, A. A. (2005) The crystal structure of a quercetin 2,3-dioxygenase from *Bacillus subtilis* suggests modulation of enzyme activity by a change in the metal ion at the active site(s). *Biochemistry 44*, 193-201.

21. Schaab, M. R. (2006).

Chapter 2

THE ROLES OF THE METAL-BINDING SITES

INTRODUCTION

Both the bacterial and the fungal examples of quecerin 2,3-dioxygenase (quercetinase) contain two cupin domains each (22,23). A significant difference between these two quercetinases is the number of metal-binding sites in each enzyme. The enzyme found in *Bacillus subtilis* (BsQueD) contains the 3His-1Glu binding domain twice within each monomer, and quantitative metal analysis by ICP-MS has shown that the over-expressed enzyme contains 1.8 moles of manganese (II) per mole of monomer (24) The fungal quercetinase (AQueD), by contrast, lacks the residues necessary for metal binding at the C-terminal cupin domain, and experimentally the enzyme contains approximately 1 mole of copper (II) per mole of monomer (25 (FIG. 2.1)). Having two nearly identical binding domains leads to an interesting question about the activity of the bacterial quercetinase: Are both metal-binding sites truly active sites? Or is it possible that only one metal-binding site is contributing to the catalytic activity of the enzyme? To better understand the role of each metal-binding site of BsQueD during catalysis, site-directed mutagenesis has been performed to diminish or eliminate metal binding at either the N-terminal or C-terminal domain.

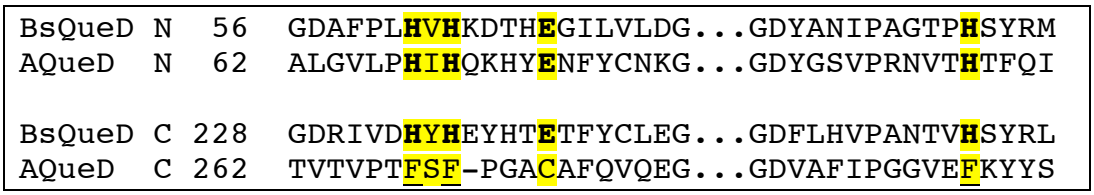

FIG 2.1: **Sequence alignment of AQueD and BsQueD**. The four metal ligands at each terminus are shown in bold. The C-terminus of AQueD contains Phe rather than His, and therefore cannot ligate a metal in the C-terminal cupin domain (26).

METHODS OF MUTAGENESIS

*Phusion® Polymerase Mutagenesis***.** One mutagenesis method was used as described by Finnzymes (27). Two 5'-phosphorylated primers are designed adjacent to one another, and one of them contains a specific mutation. They can then elongate the entire length of the plasmid in opposite directions introducing the desired mutation. Because the primers are phosphorylated, after several rounds of PCR have been completed, T4 DNA ligase is used to circularize the mutated plasmid, and it is transformed in *E. coli* for expression. Parent plasmid is at such low concentration that it will not be taken up by the cells (FIG. 2.2).

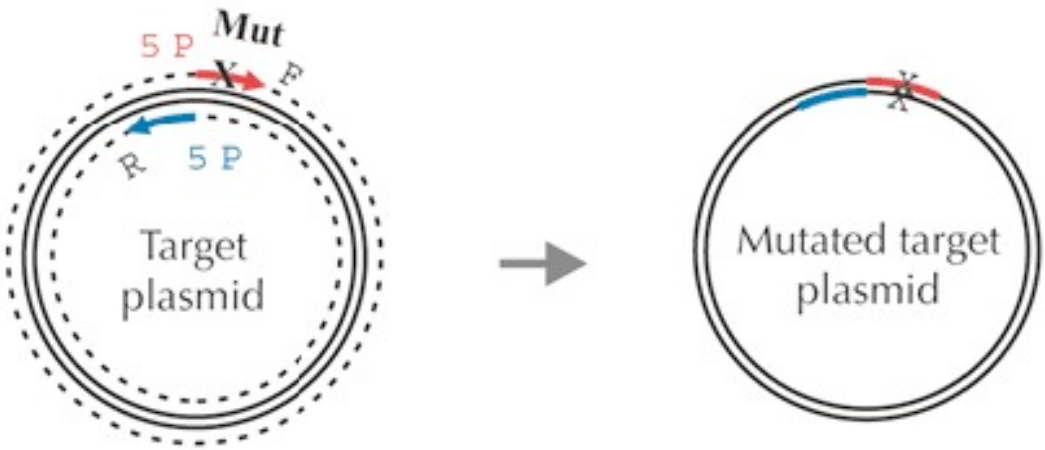

FIG. 2.2: **A cartoon representation of the phusion® polymerase mutagenesis technique**. Phosphorylated primers are designed adjacent to one another, so once extended they can be ligated to form a mutated plasmid. (Image is from Phusion® polymerase mutagenesis protocol.)

*Overlap Extension Mutagenesis***.** A second method of site-directed mutagenesis was used to prepare several of the mutants (28). This method involves a multi-step PCR followed by digestion and ligation into an empty plasmid vector. While designing primers, the gene is split into two fragments: a front segment and a back segment. These two fragments overlap in the middle of the gene at the location of the desired mutation. So that when the products of the first round of PCR are combined and cycled through a second round of PCR, they will elongate to produce the entire length of the gene.

For the first round of PCR, two sets of primers are designed-one set produces the front segment and a second set produces the back segment. The

inner primers of each set overlap one another with a T_m of at least 60 ˚C. The inside primers from each set also include at least one point mutation. (If the mutation occurs within the overlapping segment of the two inner primers, then both primers will contain the point mutation.) Because some portion of the inner primers of each set are complementary, they can act as primers for one another in the second round of PCR.

After each reaction mixture is purified to rid the solutions of all primers. A second round of PCR is performed, without template, but with equal amounts of the primer-free front and back segments from the first round of PCR. These segments can then prime one another and elongate to produce a full-sized, mutated fragment (FIG. 2.3). The outer primers of each PCR set are designed to contain restriction sequences, so that the fragment can be digested with two different restriction enzymes to be ligated into digested vector. After ligation, the plasmid is transformed in *E. coli* for expression.

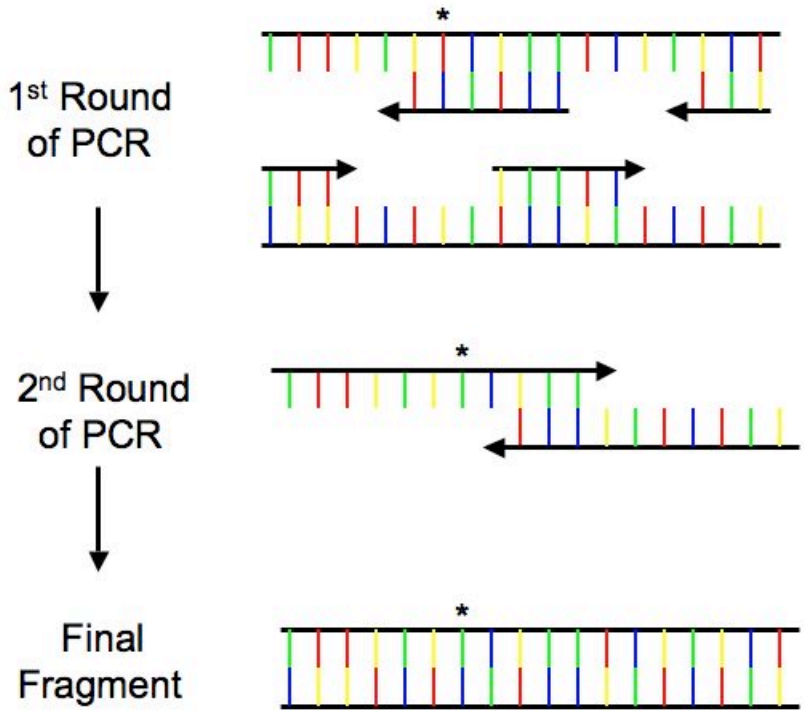

FIG. 2.3: **A schematic of the overlapping extension mutagenesis technique**. Primers are designed to produce two fragments of the gene in a first round of PCR. The inside primer of one of these reactions contains a point mutation. During a second round of PCR the front and back segments act as primers for one another and elongate to make a double-stranded, mutated fragment, which comprises the gene in its entirety. Each end of the fragment contains a restriction enzyme sequence, so that once extended, the full-length fragment can be digested and ligated into digested vector plasmid.

MATERIALS AND METHODS

Specific kits listed were used as directed by the manufacturer. Luria-Bertani (LB) brother was obtained from EMD. Protein concentration was measured with Quick Start ô Bradford Reagent (Bio-Rad) with bovine serum albumin as a standard (Pierce). Sodium dodecyl sulfate-polyacrylamide gel electrophoresis (SDS-PAGE) was performed using equipment and reagents from Bio-Rad. The proteins were visualized with Coomassie Brilliant Blue R-250 (Bio-Rad). Plasmid purifications were done with the QIAprepÆ Spin miniprep kit (Qiagen). DNA isolations from PCR reactions and agarose gels were performed with the WizardÆ SV gel and PCR clean-up system (Promega). The parent plasmid, pQuer4, was constructed previously by Dr. Brett Bareny. Taq DNA polymerase was obtained from Eppendorf, and Phusion® DNA polymerase was obtained from Finnzymes. Nucleotides were from a Promega dNTP mix. T4 DNA ligase was purchased from Invitrogen. All restriction enzymes are FastDigest® Enzymes from Fermentas Life Sciences. DNA was visualized on agarose gels with SYBR®Safe DNA gel stain purchased from Invitrogen. The plasmid vector, pET30a(+) was obtained from Novagen, and *Escherichia coli* DH5α competent cells were from Life Technologies, and *E. coli.* OneShot® TOP10, and BL21(DE3) competent cells were purchased from Invitrogen. Isopropyl-1-thio-β-D –galactopyranoside (IPTG) was obtained from Gold Biotechnology, INC. Protein isolations were performed with His-Bind®

Fractogel® Resin purchase from Novagen and columns purchase from Bio-Rad. All other chemicals and reagents were of the highest purity available (Sigma-Aldrich). All primers were synthesized with any modifications and purified by standard desalting by Integrated DNA Technolgies (IDT (TABLE. 2.1)).

TABLE. 2.1

Site-directed mutagenesis primers

H62F-H64F 9 GGA GAT GCC TTT CCG CTT TTC GTC TTC AAG GAC ACA CAT GAA GG 10 CCT TCA TGT GTG TCC TTG AAG ACG AAA AGC GGA AAG GCA TCT CC W40 GGG GTA CCT GGT CTA AAT TGG AGG AAG CG W41 CGG GAT CCG GTG TCA GGC CGG CAT G H62F 13 GTC CTT GTG GAC GAA AAG CGG AAA GGC ATC TCC 14 GCC TTT CCG CTT TTC GTC CAC AAG GAC W40 See Above W41 See Above H234F-H/236F 25 5Phos-TTT AGG GCC TTC AGA TGA TAC GAC GAT AAA CT 26 5Phos-GGT GAC CGA ATC GTT GAT TTC TAC TTT GAA TAT CAT H62A-H64A 27 5Phos-TTC CGC TTG CCG TCG CCA AGG ACA 28 5Phos-AGG CAT CTC CTT TTC CCC CG 6xHis-E69H 33 GGA CAC ACA TCA CGG AAT TCT CG 34 CCA AAA CGA GAA TTC CGT GAT GTG TG W43 GTG AGC GGA TAA CAA TTC CCC TC W44 GCC AAC TCA GCT TCC TTT CGG G

6xHis-H62A-H64A
27 5Phos-TTC CGC TTG CCG TCG CCA AGG ACA
28 5Phos-AGG CAT CTC CTT TTC CCC CG

6xHis-H234A-H236A
41 5Phos-TTT AGG GCC TTC AGA TGA TAC GAC GAT AAA CT
42 5Phos-GGT GAC CGA ATC GTT GAT GCC TAC GCT GAA TAT CAT

6xHis-E241H
45 5Phos-CA TAC ACA CAC ATT TTA TTG CCT TGA AGG CC
46 5Phos-AT ATT CAT GGT AGT GAT CAA CGA TTC GGT C

H62F-H64F, H62F. The mutants H62F-H64F and H62F were prepared by overlapping extension mutagenesis from the parent plasmid, pQuer4. For the first round of PCR, two 50 µL reactions were prepared on ice. The front segment reaction contained primers W40 and 10 for H62F-H64F or W40 and 13 for H62F, and the back segment reaction contained primers W41 and 9 for H62F-H64F or W41 and 14 for H62F. Eppendorf Taq polymerase was used for elongation, and the thermal cycler program used was called SEQ and is outlined in TABLE. 2.2.

TABLE. 2.2

PCR thermal cycler program SEQ

Temperature	Time	Number of Cycles
94˚ C	2 min	1
94˚C	20 sec	25
55˚C	20 sec	
65˚C	1 min 20 sec	

PCR products from the front segment and back segment reactions were diluted 1:10 with DI water, and used as template/primers for the second PCR reaction under the same thermal cycling conditions as reaction 1. Full-length fragments and pET30a(+) vector were digested sequentially with BamHI and KpnI for 1 h at 37 ˚C. Digestion mixtures were speedvapped to dryness, and DNA was resuspended in 9 μL autoclaved DI water. They were then combined and ligated with T4 DNA ligase for 1 h at 22 ˚C. Chemically competent *E. coli* DH5α were transformed by heat shock with ligated DNA for storage for storage, followed by the transformation by heat shock of chemically competent *E. coli* BL21(DE3) cells with plasmid isolated from the storage line.

*6xHis-E69H***.** The mutant 6xHis-E69H was prepared by the overlapping extension mutagenesis technique with the template, His-wt (preparation described in chapter 3). For the first round of PCR, the primers W43 and 34 were used to

produce the front segment, and primers W44 and 33 were used to make the back segment. Phusion® DNA polymerase was used to elongate the DNA under the thermal cycling conditions in program JAN13 (TABLE. 2.3).

TABLE. 2.3

Program JAN13

Temperature	Time	Number of Cycles
98 ˚C	30 sec	1
98 ˚C	5 sec	25
64 ˚C-72 ˚C	10 sec	
72 ˚C	10 sec	
72 ˚C	5 min	1

Successful reactions were confirmed with a 1% agarose gel. The best amplified front and back segment reactions were purified with the Promega kit and then combined for the second round of PCR, which was cycled according to program MAR26 (TABLE. 2.4).

TABLE. 2.4

Program MAR26

Temperature	Time	Number of Cycles
98 ˚C	30 sec	1
98 ˚C	5 sec	40
52 ˚C-68 ˚C	10 sec	
72 ˚C	5 sec	
72 ˚C	5 min	1

Again successful amplification was confirmed with a 1% agarose gel, and the best amplified reaction was chosen for a double digestion with kpn1 and BamHI. Digested pET30a(+) and digested full-length fragment were purified from a 1% agarose gel with the Promega kit. Pure DNA was then combined and incubated overnight at 16 ˚C with T4 DNA ligase. Chemically competent *E. coli.* OneShot® TOP10 and BL21(DE3) cells were transformed by heat shock with the ligated DNA.

*H234F-H236F, H62A-H64A, 6xHis-H62A-H64A, 6xHis-H234A-H236A, and 6xHis-E241H***.** Four mutations were made using the Phusion® polymerase mutagenesis protocol (6). H234F-H236F (primers 25 and 26) and H62A-H64A

(primers 27 and 28) both modified the template pQuer4. H234F-H236F was cycled through program E (TABLE. 2.5), and H62A-H64A was cycled on program 528 (TABLE. 2.6).

TABLE. 2.5

Program E

Temperature	Time	Number of Cycles
98 ˚C	30 sec	1
98 ˚C	5 sec	25
70 ˚C-76 ˚C	2 min	
72 ˚C	1 min	1

TABLE. 2.6

Program 528

Temperature	Time	Number of Cycles
98 ˚C	30 sec	1
98 ˚C	10 sec	25
60.5 ˚C	25 sec	
57 ˚C-72˚C	2 min 45 sec	
72 ˚C	5 min	1

The His-wt template (preparation described in chapter 3) was used to create the 6xHis-H62A-H64A (primers 27 and 28), 6xHis-H234A-H236A (primers 41 and 42) mutations, and 6xHis-E241H (primers 45 and 46). 6Hix-H234A-H236A and 6xHis-E241H were cycled on program E (TABLE. 2.5). 6xHis-H62A-H64A was cycled on program NOV21 (TABLE. 2.7). Three different amounts of template were tested to produce the mutation with the lowest amount of parent plasmid in the product mixture.

TABLE. 2.7

Program NOV21

Temperature	Time	Number of Cycles
98 ˚C	30 sec	1
98 ˚C	7 sec	25
65.8 ˚C	20 sec	
72 ˚C	1 min 30 sec	
72 ˚C	5 min	1

After mutagenic amplification, each of the four mutations were incubated overnight at 16 ˚C with T4 DNA ligase. Then chemically competent *E. coli.* OneShot® TOP10 and BL21(DE3) cells were transformed by heat shock with the ligated DNA.

Mutant Expression Experiments. Expression of mutant enzyme was confirmed by growing 100 mL LB cultures with 30 mg/L kanamycin at 37 ˚C with 200 rpm shaking to an OD600 of 0.6-09. Cultures were then induced with 50 mg/L IPTG and 1 mM MnCl2 for four hours at 20 ˚C. Control cultures were supplemented with 1 mM MnCl2 and shaken for four hours at 20 ˚C, but they were not exposed to IPTG. Cells were harvested by centrifugation at 20,000 xg for 20 minutes in a Sorvall RC 5C Plus centrifuge at 4 ˚C. Pellets were stored at -80 ˚C until needed.

The successful expression of the mutant proteins was analyzed by SDS-PAGE. Cells were lysed at 700 psi in a French pressure cell. Soluble and insoluble portions were separated by centrifugation at 20,000 xg for 20 minutes in a Sorvall RC 5C Plus centrifuge. Small portions of the soluble and insoluble fractions were dissolved in denaturing loading buffer

Mutant Expression for Analysis. Mutant protein was prepared as described above in five 1 L cultures of M9 minimal medium rather than 100 mL of LB.

Purification of Mutant Proteins. Cells were lysed and cell waste was centrifuged away as described above. The soluble fraction was loaded onto a HisBand® Fractogel® column conditioned with $NiSO_4$. Proteins were concentrated with a 10,000 molecular weight cut off (MWCO) concentrator (Millipore) and a Centra-CL2 swinging bucket rotor centrifuge 9international

Equipment Company). Protein concentration was determined by Bradford assay with BSA standards or nanodrop.

Inductively Coupled Plasma Mass Spectrometry (ICP-MS)**.** Samples were prepared for inductively couple mass spectrometry (ICP-MS) by first removing exogenously bound metals with a chelex-100 column. Samples were then acidified in 10% ultrapure nitric acid and heated for 15 min at 45 ˚C. Each sample was then diluted to yield between 0.1 and 30 ppb metal in 10 mL of solution and sent to Dr. Panjai Prapaipong for analysis by ICP-MS.

RESULTS

Site directed mutagenesis by overlapping extension was successfully employed to mutate two residues in the N-terminal binding domain creating the mutant enzyme His62F-His64F. Figure 2.4 is a 1% agarose gel, which contains a 250 bp forward fragment, a 1300 bp back fragment and the full length extended fragment (FIG. 2.4).

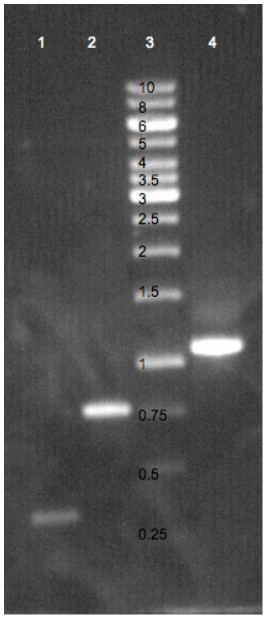

FIG. 2.4: **1% agarose gel of the products of the first and second rounds of PCR for the H62F-H64F mutation.** Lane 1: front segment produced by primers Wilson 40 and Oligo 10; Lane 2: back segment produced by primers Wilson 41 and Oligo 9; Lane 3: Fermentas GeneRulerô 1 kb DNA ladder, 5 µL. Sizes of DNA standards are labeled and reported in Kb; Lane 4: full length segment produced by annealing and elongating the products from each reaction of the first round of PCR.

Expression of mutant enzyme was verified by comparing cell lysate of induced cultures to the cell lysate of control (non-induced) samples on a 12% SDS-PAGE gel (FIG. 2.5). Mutant protein is only present in the insoluble fraction of the induced culture.

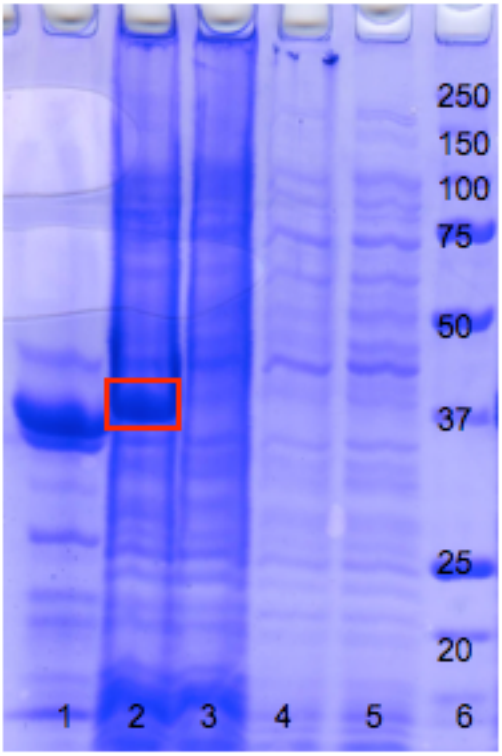

FIG. 2.5: **12% SDS-PAGE gel contains cell lysate from induced and control (non-induced) cultures of H62F-H64F**. Lane 1: purified wild type enzyme; Lane 2: induced sample cell pellet; Lane 3: control (non-induced) sample cell pellet; Lane 4: induced sample soluble fraction; Lane 5: control sample soluble fraction; Lane 6: Biorad Precision Plus Proteinô standard ladder, 15 µL. Sizes of the protein standards in lane 1 are labeled and reported in kDa.

Do to the lack of soluble H62F-H64F mutant protein, a second more conservative mutant was designed, H62F. The wild type DNA was successfully amplified with mutant primers as evidenced on a 1% agarose gel (FIG. 2.6).

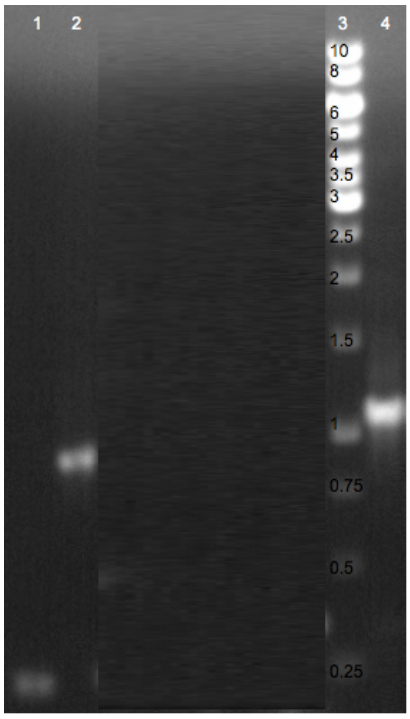

FIG. 2.6: **1% agarose gel of the first and second PCR products for the H62F mutation**. Lane 1: front segment produced by primers Wilson 40 and Oligo 13, Lane 2: back segment produced by primers Wilson 41 and Oligo 14; Lane 3: Fermentas GeneRulerô 1 kb DNA ladder, 5 µL. Sizes of DNA standards are labeled and reported in Kb; Lane 4: full length segment produced by annealing and elongating the PCR products from each reaction of the first round of PCR.

The expression of mutant, H62F, protein was confirmed by visualizing induced cultures versus control (non-induced) cultures on a 12% SDS-PAGE gel (FIG. 2.7). Again the expressed protein is clearly visible as a band in the pellet of the induced samples.

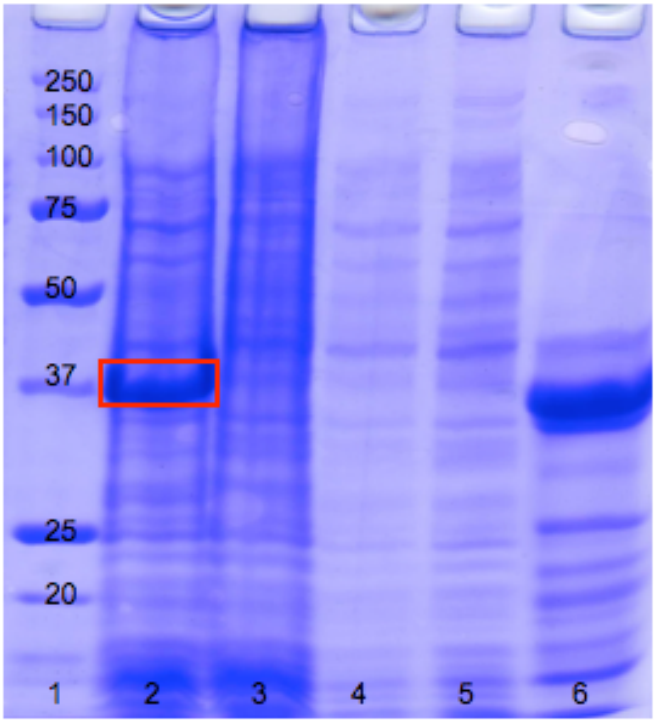

FIG. 2.7: **Expression of the mutant H62F**. This 12% SDS-PAGE gel contains Lane 1: Biorad Precision Plus Proteinô standard ladder, 15 µL Sizes of the protein standards in lane 1 are labeled and reported in kDa.; Lane 2: induced sample cell pellet; Lane 3 control (non-induced) sample cell pellet; Lane 4 induced sample soluble fraction; Lane 5: control sample soluble fraction and Lane 6: purified wild type QueD.

A C-terminal mutant, H234F-H236F, was also designed. The successful PCR is shown as FIG. 2.8.

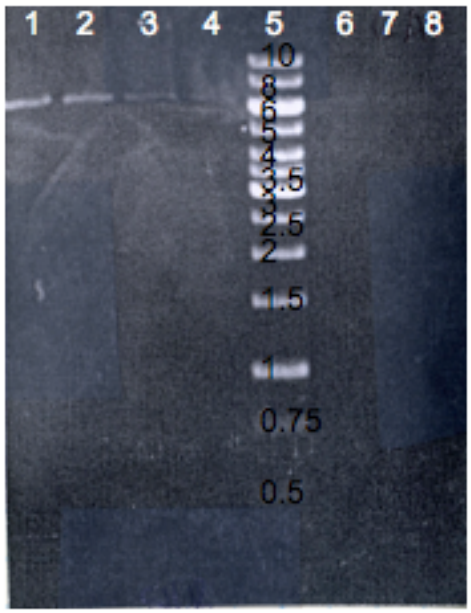

FIG. 2.8: **1% agarose gel containing the PCR product H234F-H236F**. Lane: 70.0 ˚C; Lane 2: 70.5 ˚C; Lane 3: 71.3 ˚C; Lane 4: 72.4 ˚C; Lane 5: Fermentas GeneRulerô 1 kb DNA ladder, 5 µL. Sizes of DNA standards are labeled and reported in Kb; Lane 6: 73.8 ˚C; Lane 7: 74.9 ˚C; Lane 8: 76.0 ˚ C.

The expression of the C-terminal mutants was confirmed on a 12% SDS-PAGE gel (FIG. 2.9). As with the N-terminal mutants, the protein is clearly visible as a band in the insoluble portion of the induced cultures, but no band is detected in the soluble portion.

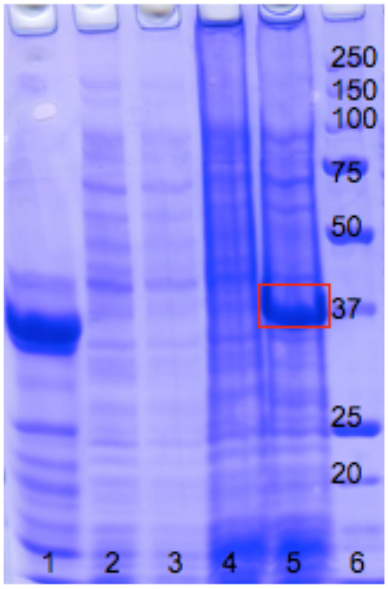

FIG. 2.9: **12% SDS-PAGE gel of expression of mutant H234F-H236F**. Lane 1: purified wild type control; Lane 2: control (non-induced) sample soluble fraction; Lane 3: induced sample soluble fraction; Lane 4: control (non-induced) sample cell pellet; Lane 5 induced sample cell pellet; Lane 6: Biorad Precision Plus Proteinô standard ladder, 15 µL Sizes of the protein standards in lane 1 are labeled and reported in kDa.

The program T-Coffee was used to perform a multiple sequence alignment was conducted with several cupin enzymes: two from the organism *Bacillus subtilis* (oxalate decarboylase (Oxd C)) and quercetin 2,3-dioxygenase), one from *Pseudomonas putida*, one from *Streptomyces* sp. FLA, and one from *Aspergillus flavus* (AQueD (29)). The cupin domains at both termini for BsQueD and AQueD are shown in FIG. 2.10.

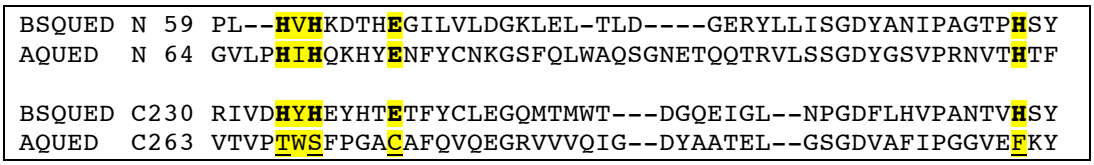

FIG. 2.10: **T-Coffee alignment of AQueD and BsQueD**. The program Chimera was used to conduct a second sequence alignment of BsQueD and *Aspergillus japonicus* to ensure that mutated residues are in fact similar to the C-terminal residues of AQueD.

Previous mutant designs were based on the assumption that phenylalanine in the fungal quercetinase was aligned sequentially with metal-binding histidines in the bacterial quercetinase. Armed with the current sequence alignment, a more conservative mutation scheme was developed. Rather than mutating histindines to phenylalanines, they were successfully mutated to alanines (FIG. 2.11.)

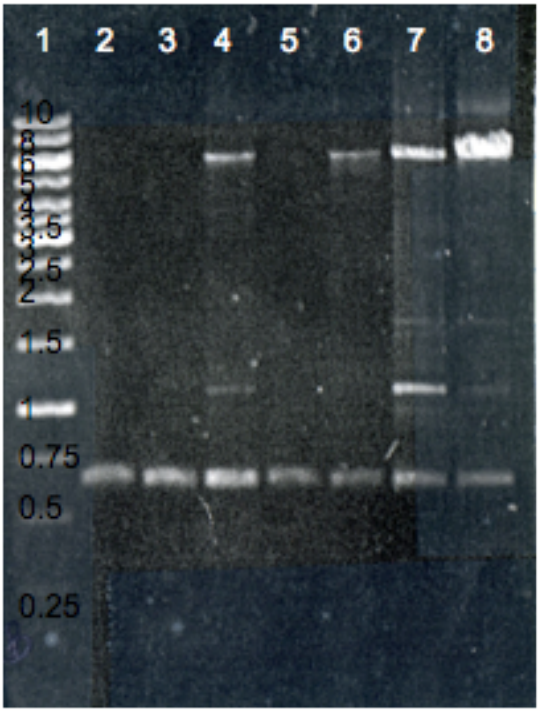

FIG. 2.11: **1% agarose gel of the optimization of the PCR reaction to produce the mutant H62A-H64A**. Lane 1: Fermentas GeneRulerô 1 kb DNA ladder, 5 µL. Sizes of DNA standards are labeled and reported in Kb; Lane 2: 57.0 ˚C; Lane 3: 58.1 ˚C; Lane 4: 60.2 ˚C; Lane 5: 63.0 ˚C; Lane 6: 66.3 ˚C; Lane 7: 69.1 ˚C; Lane 8: 71.0 ˚C.

Unfortunately, this mutation also yielded insoluble protein (FIG. 2.12).

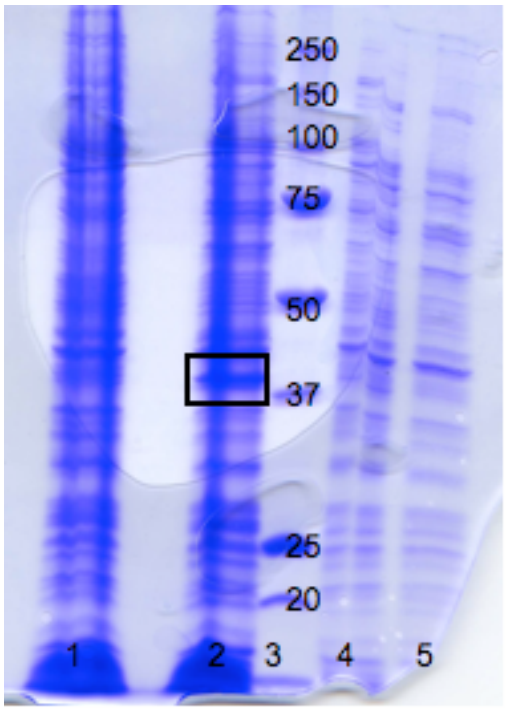

FIG. 2.12: 12% **SDS-PAGE gel of the expression of the mutant H62A-H64A**. Lane 1: control (non-induced) sample cell pellet; Lane 2: induced cell pellet; Lane 3: Biorad Precision Plus Proteinô standard ladder, 15 µL Sizes of the protein standards in lane 1 are labeled and reported in kDa; Lane 4: control (non-induced) sample soluble fraction; Lane 5: induced soluble fraction.

The fourth metal-binding residue, Glu69, was also mutated at the N-terminal domain. The successful PCR products of mutation E69H are shown in Figures 2.13 and 2.14. This particular mutation was produced from a His-tagged template (chapter 3).

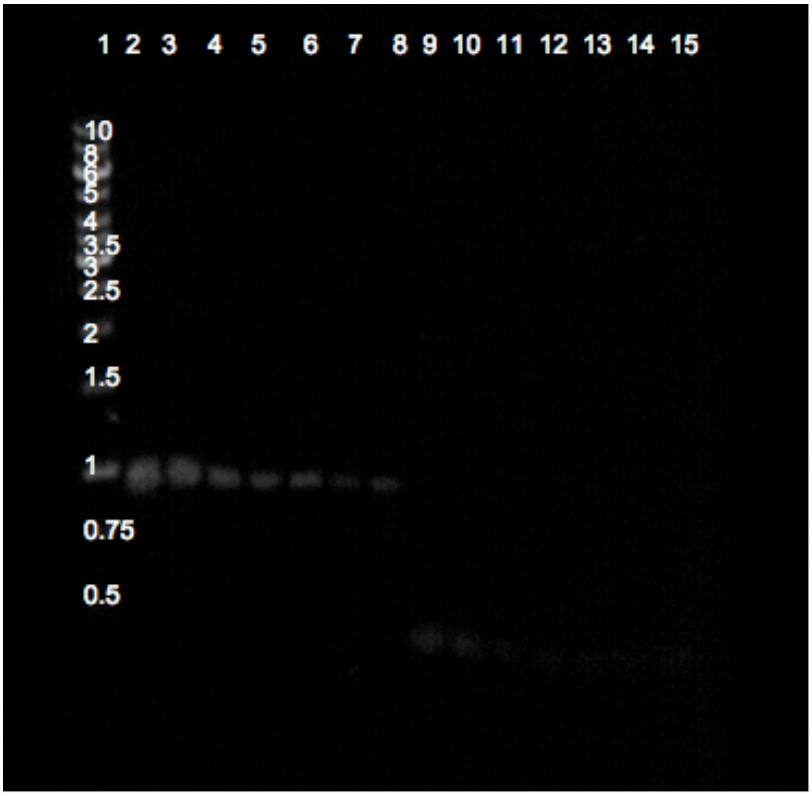

FIG. 2.13: **1% agarose gel of the first round of PCR producing the front fragment of 6xHis-E69H.** This was produced with primers Wilson 43 and Oligo 34 and the back fragment with primers Wilson 44 and Oligo 33 for the E69H mutation. Lane 1: Fermentas GeneRulerô 1 kb DNA ladder, 5 µL. Sizes of DNA standards are labeled and reported in Kb; Lanes 2-8: products of the PCR reaction producing the back fragment at varying temperatures Lane 2: 64.6 ˚ C; Lane 3: 65.7 ˚C; Lane 4: 67.2 ˚ C; Lane 5: 69.0 ˚C; Lane 6: 70.5 ˚C; Lane 7: 71.5 ˚C; Lane 8: 72.0 ˚C; Lanes 9-15: products of the PCR reaction producing the front fragment at varying temperatures Lane 9: 64.6 ˚C; Lane 10: 65.7 ˚C; Lane 11: 67.2 ˚C; Lane 12: 69.0 ˚C; Lane 13: 70.5 ˚C; Lane 14: 71.5 ˚C; Lane 15: 72.0 ˚C.

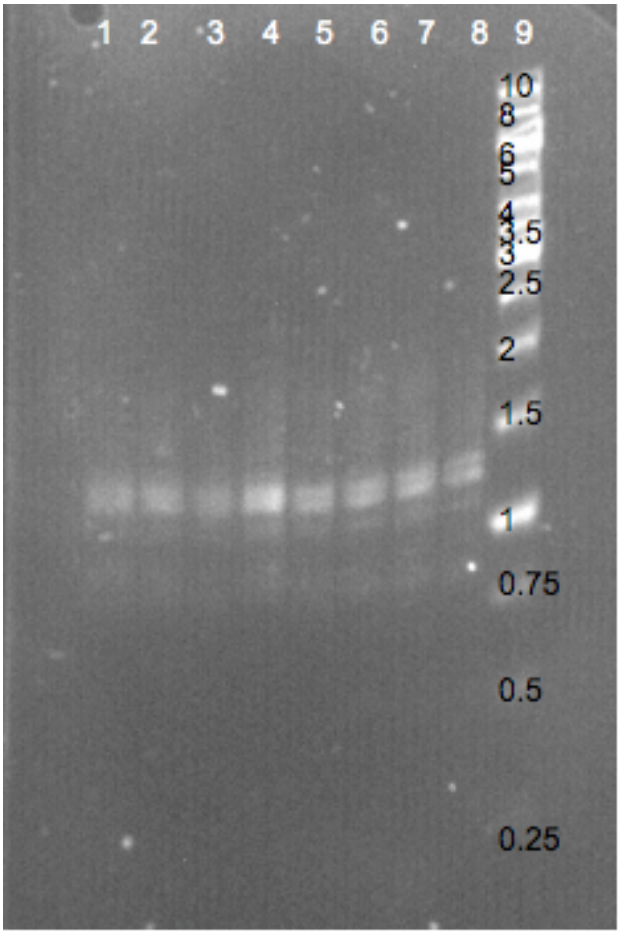

FIG. 2.14: **1% agarose gel of the product of the second PCR reaction to produce the mutation 6xHis-E69H**. Lane 1: 72.0 ˚C; Lane 2: 71.5 ˚C; Lane 3: 70.5 ˚C; Lane 4: 69.0 ˚C; Lane 5: 67.2 ˚C; Lane 6: 65.7 ˚C; Lane 7: 64.6 ˚C; Lane 8: 64.0 ˚C; Lane 9: Fermentas GeneRulerô 1 kb DNA ladder, 5 µL. Sizes of DNA standards are labeled and reported in Kb.

The E69H mutation successfully produced soluble protein. Also, the purification of the mutant was successful without the standard activity assay because the protein is fused with a hexahistidine tag (FIG. 2.15.)

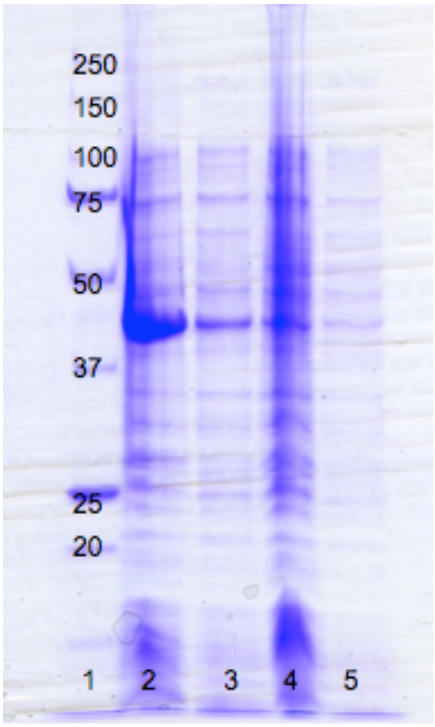

FIG. 2.15: **12% SDS-PAGE gel of the 6xHis-E69H mutant**. Lane 1: Biorad Precision Plus Proteinô standard ladder, 15 µL. Sizes of the protein standards in lane 1 are labeled and reported in kDa; Lane 2: induced sample cell pellet; Lane 3: induced sample soluble fraction; Lane 4: control (non-induced) sample cell pellet; Lane 5: control (non-induced) sample soluble fraction.

It was unclear whether the 6xHis tag was responsible for the sudden expression of soluble mutant protein, or if it was simply because of the selected amino acid change, so the H62A-H64A mutation was also attempted with the 6xHis-BsQueD template (FIG. 2.16.) And it appeared that a small amount of protein was expressed for each (FIG. 2.17 and FIG. 2.19).

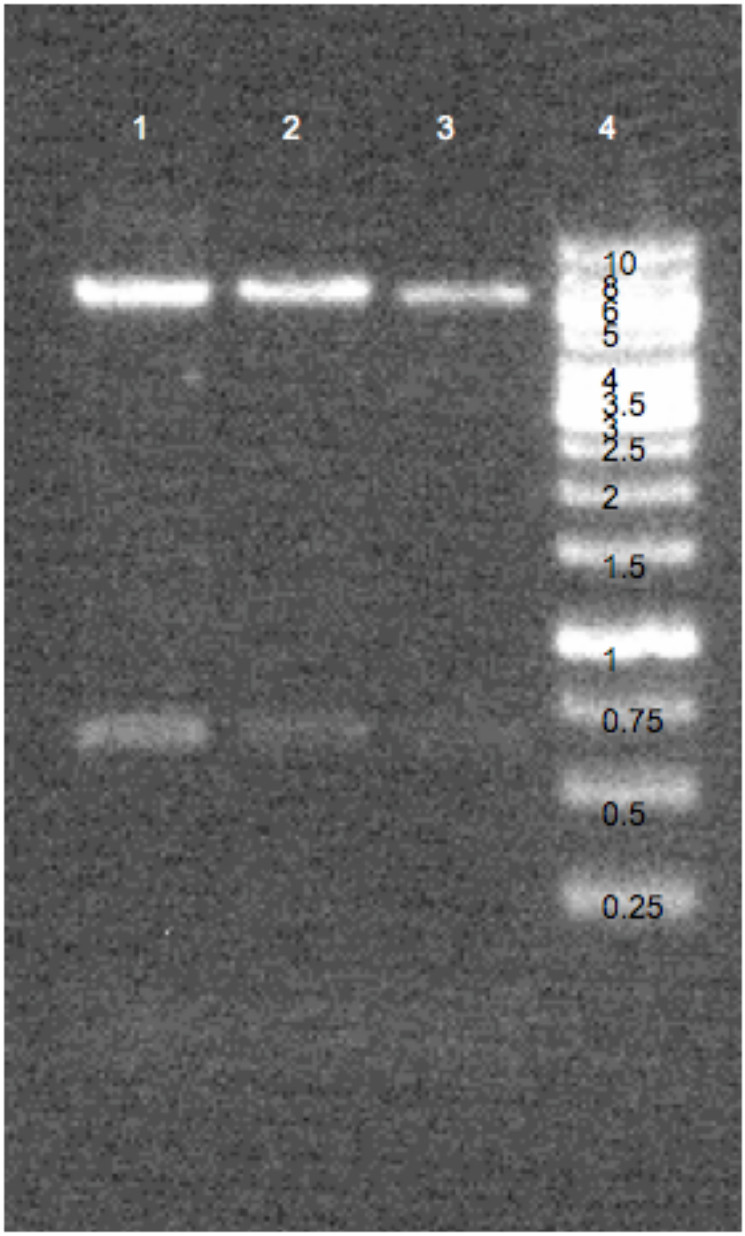

FIG. 2.16: **1% agarose gel of the 6xHis-H62A-H64A mutant**. This was made using varied amounts of template for phusion polymerase PCR reaction. Lane 1: 20 µL template; Lane 2: 10 µL template; Lane 3: 5 µL template; Lane 4: Fermentas GeneRulerô 1 kb DNA ladder, 5 µL. Sizes of DNA standards are labeled and reported in Kb.

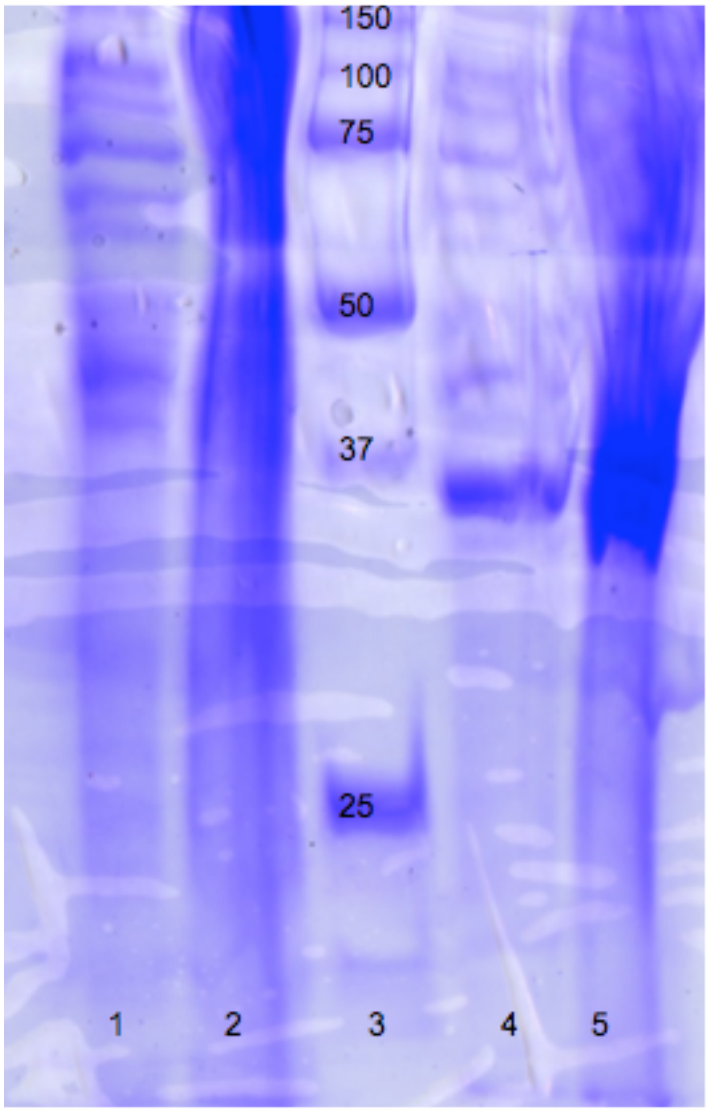

FIG. 2.17: **12 % SDS-PAGE gel of the 6xHis-H62A-H64A mutant**. Lane 1: control (non-induced) sample soluble fraction; Lane 2: control (non-induced) sample cell pellet; Lane 3: Biorad Precision Plus Proteinô standard ladder, 15 µL. Sizes of the protein standards in lane 1 are labeled and reported in kDa; Lane 4: induced sample soluble fraction; Lane 5: induced sample cell pellet.

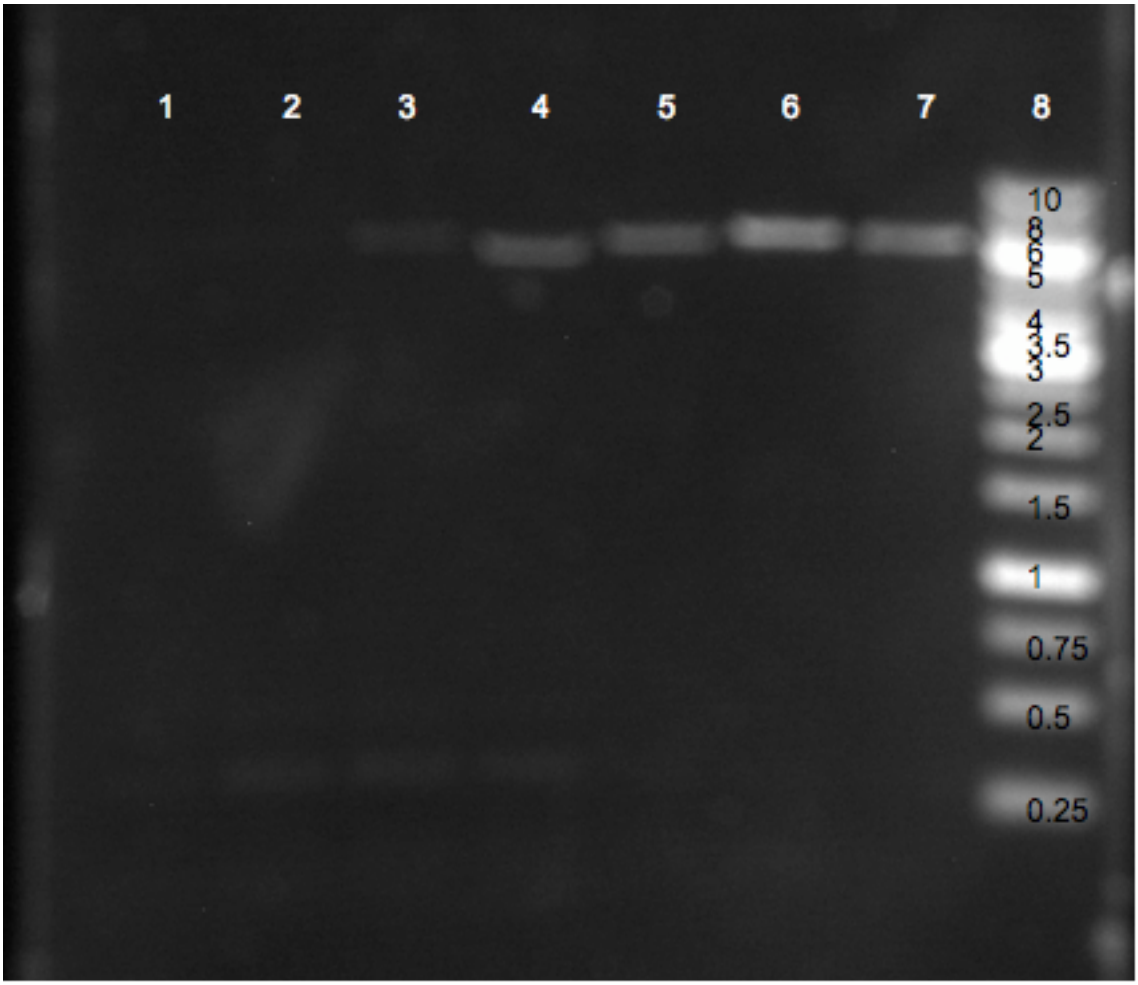

FIG. 2.18: **PCR product of the 6xHis-H234A-H236A mutant**. This was made using primers oligo 41 and oligo 42 and the phusion polymerase mutagenesis technique at various temperatures. Lane 1: 66.9 ˚C; Lane 2: 64.8 ˚C; Lane 3: 61.9 ˚C; Lane 4: 58.3 ˚C; Lane 5: 55.4 ˚C; Lane 6: 53.2 ˚C; Lane 7 52.0 ˚C; Lane 8: Fermentas GeneRulerô 1 kb DNA ladder, 5 µL. Sizes of DNA standards are labeled and reported in Kb.

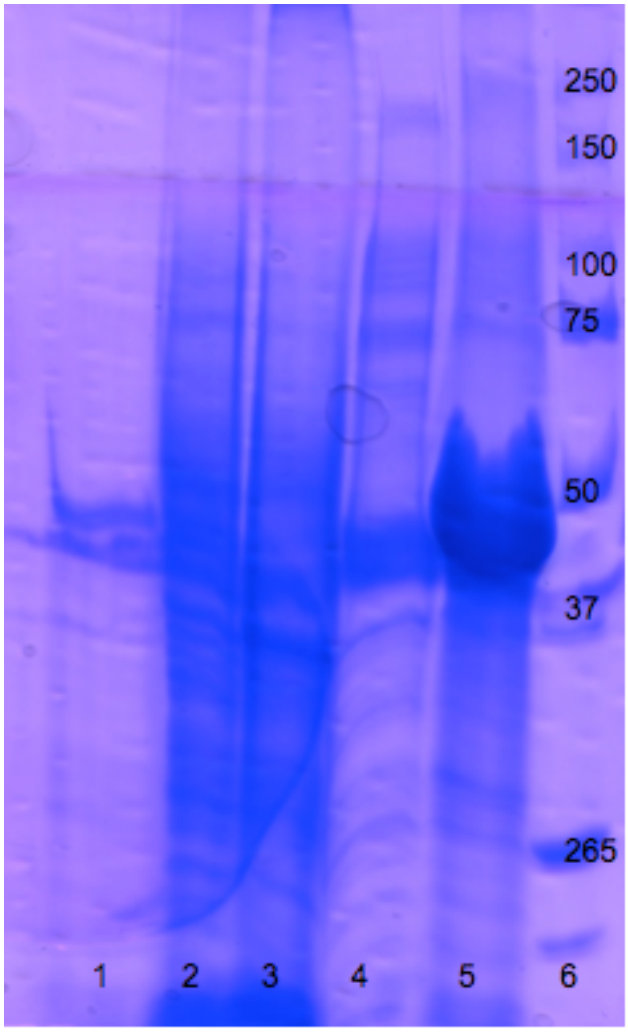

FIG. 2.19: **12% SDS-PAGE gel of the 6xHis-H234A-H236A mutant**. Lane 1: purified His tagged wild type enzyme; Lane 2: control (non-induced) sample soluble fraction; Lane 3: control (non-induced) sample cell pellet; Lane 4: induced sample soluble fraction; Lane 5: induced sample cell pellet; Lane 6: Biorad Precision Plus Proteinô standard ladder, 15 µL. Sizes of the protein standards in lane 1 are labeled and reported in kDa.

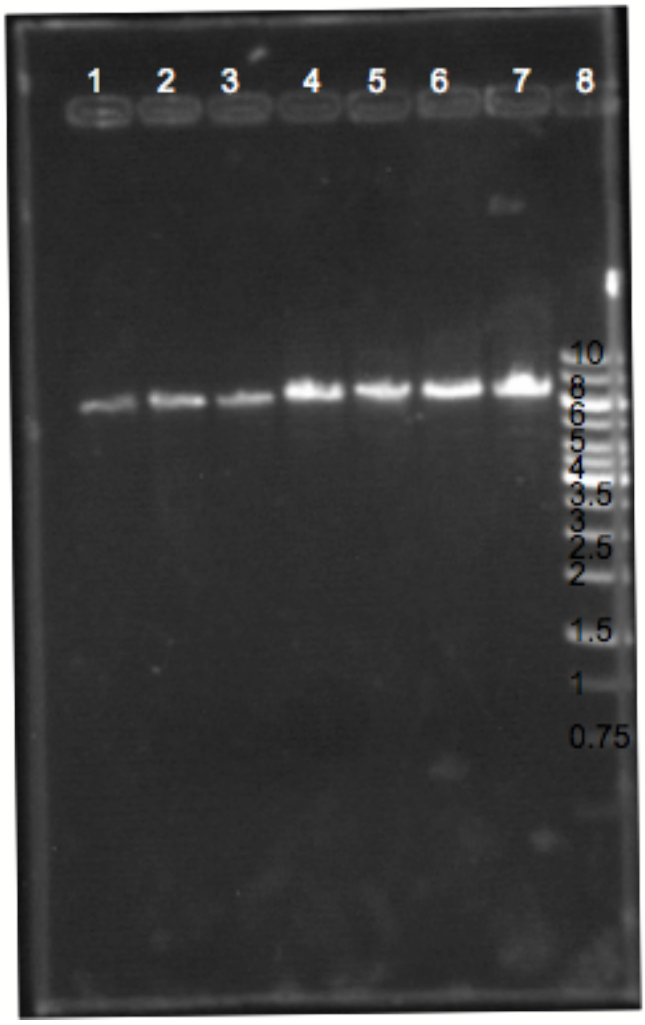

FIG. 2.20: **1% agarose gel of the PCR product of the phusion polymerase mutagenesis product of 6xHis-E241H**. Lane 1: 57.0 ˚C; Lane 2: 58.1 ˚C; Lane 3: 60.2 ˚C; Lane 4: 63.0 ˚C; Lane 5: 66.3 ˚C; Lane 6: 69.1 ˚C; Lane 7: 71.0 ˚C. Lane 8: Fermentas GeneRulerô 1 kb DNA ladder, 5 µL. Sizes of DNA standards are labeled and reported in Kb.

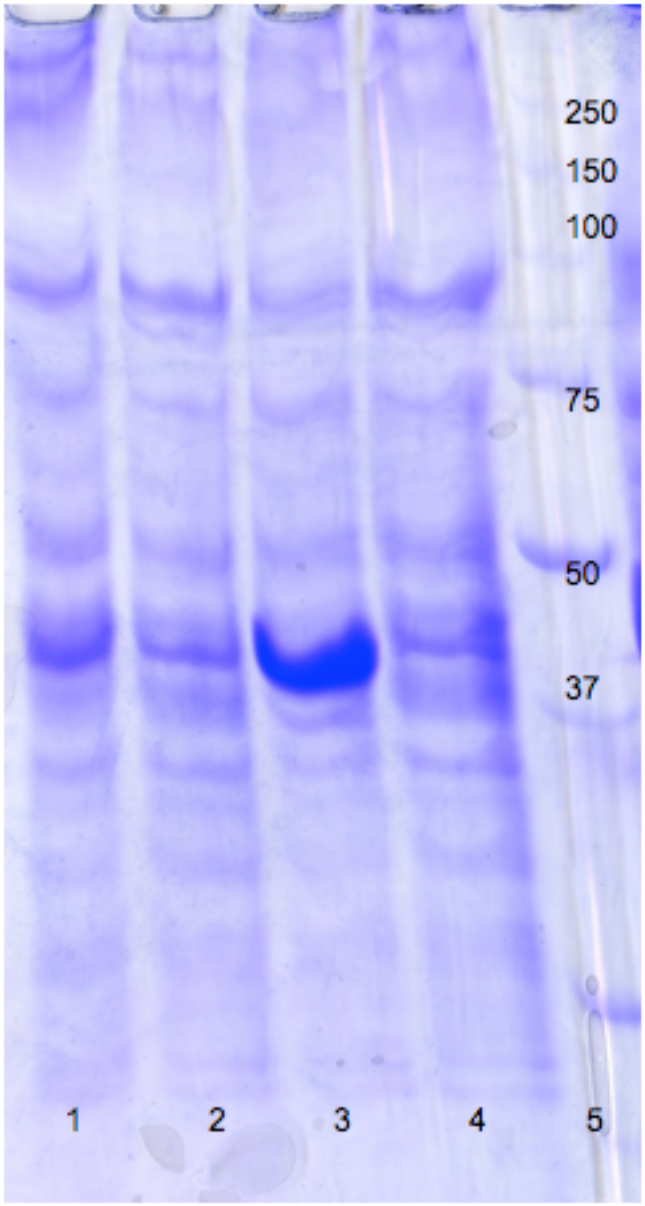

FIG. 2.21: **12% SDS-PAGE gel of the expression of the mutant 6xHis-E241A**. Lane 1: induced sample soluble fraction; Lane 2: control (non-induced) sample soluble fraction; Lane 3: induced sample cell pellet; Lane 4: control (non-induced) sample cell pellet; Lane 5: BioRad Precision Plus Proteinô standard ladder, 15 µL. Sizes of the protein standards in lane 1 are labeled and reported in kDa.

Further sequence alignment analysis was carried out with the program Chimera (30). Again the enzymes BsQueD, AQueD, and BsOxD were aligned, but a further step was completed. The x-ray crystallography structure of each enzyme was downloaded from the protein data bank and shown in the Chimera viewer. All residues were hidden except a few residues at the N-terminal and C-terminal metal-binding domains. With this overlap, it is very clear that the N-terminal binding residues of each of the three enzymes are very similar (FIG. 2.22), but that the residues in the C-terminal binding domain are not quite as aligned. Also the previous sequence alignment (FIG. 2.10) suggested that T, S and F correspond to the Hs in the C-terminal binding domain. The most current alignment replaces those with W, F, and F; and therefore, the less conservative H to A mutations were likely not nearly as advantages as expected.

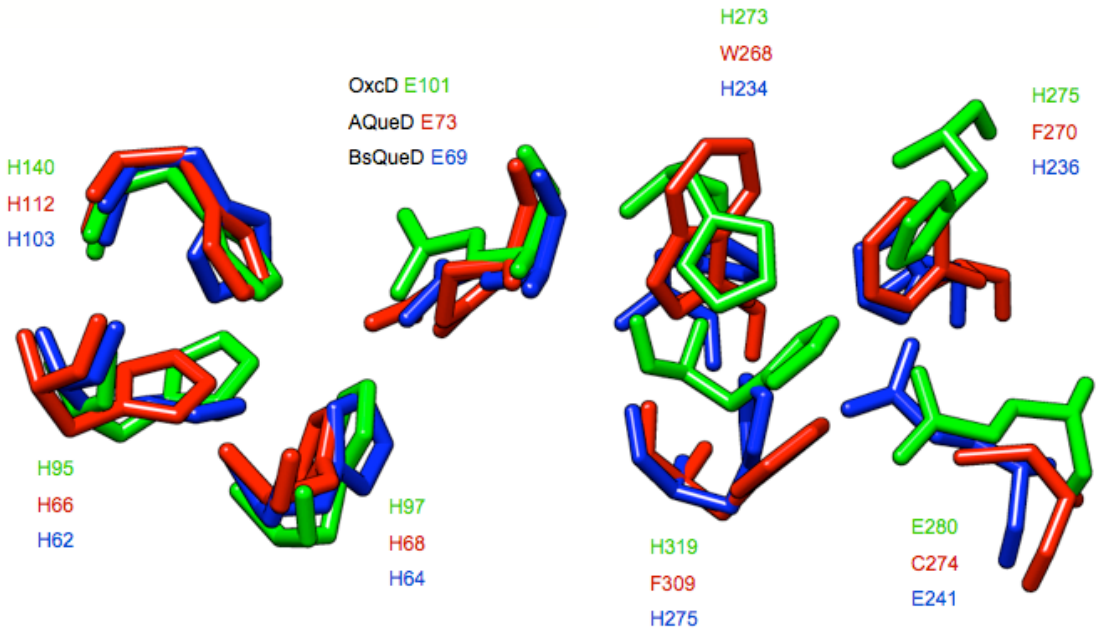

FIG. 2.22: **Structural sequence alignment**. The program Chimera was used to create spatial alignments of the metal binding sites in the N-terminal domains (left) and the C–terminal domains (right) of BsQueD (blue; PDB 1Y3T), OxdC (green; PDB 1UW8), and AQueD (red; 1JUH). The 3His1Glu motifs of all three enzymes align very well at the N-terminus, but at the C-terminus, AQueD lacks the appropriate residues for metal binding (WFFC rather than HHHE) while BsQueD's and OxdC's residues are slightly off-set from one another.

As samples were prepared for further analysis, it was noted that the typical concentration for each of the mutants was significantly lower than concentrations achieved with the wild type enzyme (TABLE. 2.8). To better

understand the solubility of the mutants, samples of E69H and H234A-H236A were concentrated for several rounds. After five rounds, E69H is 2.50 mg/mL and H234A-236A is 0.568 mg/mL. This is considerably lower than wild type concentrations making it evident that the mutated enzymes are certainly less soluble than wild type (TABLE. 2.9).

TABLE. 2.8

Comparison of the solubility of BsQueD and its mutants.

Enzyme	Average Conentration (μg/mL)
Wild Type BsQueD	18,400
H62F-H64F	279
H234F-H236F	392
E69H	719

TABLE. 2.9

Mutant protein concentrations after rounds of concentration

E69H (mg/mL)	H234A-H236A (mg/mL)
3.32	0.0100
1.94	0.184
2.01	0.277
2.41	0.416
2.50	0.568

The maximum velocities of each of the mutants were compared to wild type (TABLE. 2.10). E69H is the only mutant that has been observed to decompose quercetin, but at a rate of 5.72 x 10^{-3} mmol/min mg, it is much less active than wild type enzyme, which has a rate of 15.9 mmol/min mg. This loss in activity is much greater than the 50% loss expected by eliminating activity at one metal-binding site even when accounting for the lowered solubility of E69H. It is possible that this residue is participating in the reaction as more than just a metal-binding residue. It could be acting as a base extracting a proton from the 3-hydroxyl group of quercetin before the reaction can proceed (24). This could account for the drastic loss in activity. To better understand the role of E69 structural studies were conducted.

TABLE. 2.10

Specific activity comparison.

Protein	Specific Activity (μmol/min/mg)
WT	15.9
E69H	5.72×10^{-3}
H62A-H64A	Not Active
H234A-H236A	Not Active
E241H	Not Active

The secondary structures of the mutants were compared by circular dichorism (CD) spectroscopy. The spectra of H62A-H64A and H234A-H236A were impossible to interpret at wavelengths less than 230 nm. Samples were diluted stepwise in hopes of observing a useable signal, but the signal that was finally readable was the same as that of the buffer only control (data not shown.) However, E69H produces a signal very similar to that of the wild type enzyme (FIG. 2.23.) Therefore, it is likely that soluble E69H is folded similarly to wild type, and some other factor must be causing the decreased activity of the mutant.

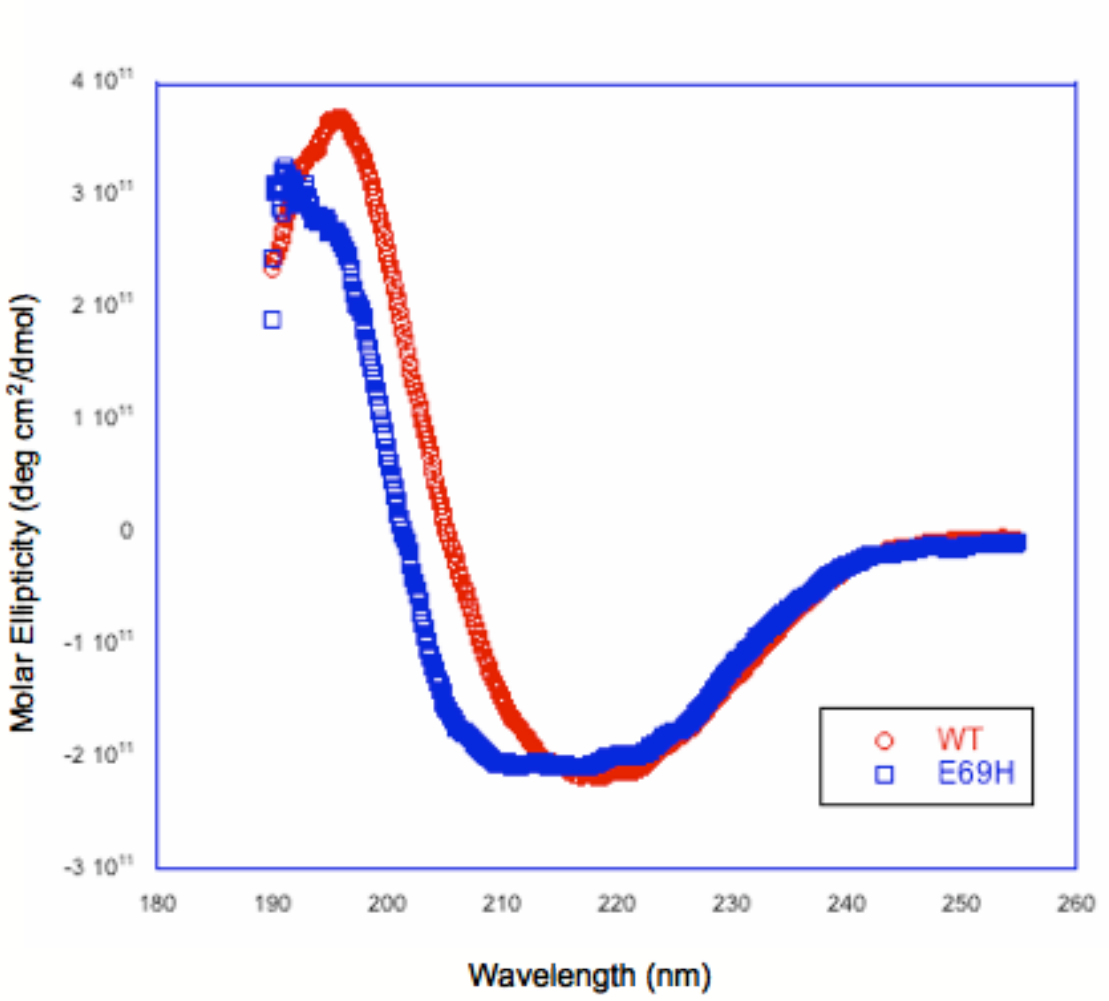

FIG. 2.23: **A structural comparison of 6xHis-BsQueD enzyme and 6xHis-E69H by CD spectroscopy**. CD spectra of 6xHis-H62A-H64A and 6xHis-H234A-H236A were impossible to interpret below 230 nm (data not shown).

Most of the mutants were analyzed for metal content by inductively coupled plasma mass spectrometry. As expected all the mutants contained less Mn(II) per molecule than the wild type enzyme. What was not expected, however, was such a great loss in metal content. The only viable mutant, E69H, contained just over 3% of the Mn(II) that is found in wild type BsQueD.

TABLE. 2.11

Comparison of metal content by ICP-MS.

Sample	mol Mn/ mol enzyme
WT	1.9
H62A-H64A	0.091
H234A-H236A	0.23
E69H	0.062

DISCUSSION

Several mutants of BsQueD have been successfully constructed. Unfortunately, the majority of these mutants have proven too insoluble for any in-depth structural or functional analysis. This difficulty obtaining soluble mutants was largely unexpected because wild type enzyme is un-aggregated under the given conditions. However, it is often the case that proteins over expressed in *E. coli* are produced as insoluble inclusion bodies. In fact, it has been estimated that as little as 13-23% of proteins over express in *E. coli* as soluble protein (31).

The addition of a 6xHis tag to create fusion mutant proteins made it possible to analyze inactive enzymes. The purification protocol of untagged enzyme involves several steps in which the activity of the enzyme is the best way to identify the protein. Also, the traditional method involves several steps; therefore, starting with a high amount of soluble, protein is more critical because there are more steps in which to lose protein. Before the addition of the fusion tag it was very difficult to purify any of the His mutants, but for His mutants fused to the 6xHis tag, it was possible to obtain enough relatively pure mutant protein for ICP MS, kinetic analysis, and CD spectroscopy. The 6xHis tag, however, has been shown to consistently decrease the solubility of proteins (32). Therefore, it is possible that for the active mutant (E69H) it may be beneficial to attempt a purification without the 6xHis tag.

During the course of this study, it was learned that a lab from the University of Florida was undertaking a similar study with oxalate decarboxylase (OxDC) from *B. subtilis* (33). Like BsQueD, OxDC is a bicupin enzyme that contains an atom of Mn(II) at each cupin domain. This group did not attempt to make changes to any histidine residues at either binding domain because in previous work with OxDC from *Flammulina velutipes* such mutations produced only inactive enzyme. They instead made several substations to the N-terminal and C-terminal glutamic acid residues (E101 and E280). While CD spectra of the mutants closely resembled that of the wild type OxDC, their E101D mutation

contained significantly less Mn(II) per molecule (0.09 compared to 1.87 in wild type). This is similar to the loss of metal-binding observed in the BsQueD mutant E69H (0.062 compared to 1.9 in wild type.) Of all the single mutations that were made, E101D contained the least amount of Mn(II). Therefore, it may be very beneficial to prepare other mutations of E69 and E241 of BsQueD to get a clearer idea of the role of the glutamic acid residues in this particular enzyme. Future mutants planned will contain A, Q, and D at the E69 and E241 positions. After each mutation the soluble expression will be optimized. As can be seen in figure 2.21, the soluble expression of E241H has yet to be successful. This may in part account for the lack of activity observed in this particular mutant, but it is also possible that the E241H mutation will produce completely inactive enzyme.

A monocupin example of quercetin 2,3-dioxygenase from *Streptomyces* sp. FLA (SQueD) has been over expressed in *E. coli* (34). After *in vivo* metal incorporation studies, it was determined that supplementation with Ni(II) and Co(II) yielded active enzyme, but no QueD activity was observed from samples supplemented with Mn(II), Fe(II), Cu(II) or Zn(II). The Co-SQueD has a similar metal incorporation and specfic activity to that of BsQueD expressed with Co(II); both have approximately 0.5 atoms of metal per molecule and their activities are 7.6 s^{-1} and 6.7 s^{-1} respectively. As a result of EPR spectroscopic analysis, this group believes that the metal does not play a redox role in the catalytic reaction, but rather the metal is acting to stabilize the substrate and its intermediates in the

binding pocket. This could explain why so many different metals (Mn, Fe, Co, Ni, and Cu) have been shown to produce active QueD enzyme. This conclusion is further strengthened by the fact that the quercetinase reaction can occur in the presence of base without any enzyme present (35).

While the metal may not be necessary for a redox reaction, the presence of metal seems to directly correlate to the activity of enzyme. Samples with lower amounts of metal per molecule (such as Fe-BsQueD or Co-SQueD) exhibit lower levels of activity than samples with higher metal incorporation (such as Mn-BsQueD or Ni-SQueD). This could be evidence that the metal is helping to stabilize the enzyme structurally rather than directly participating in the catalytic reaction.

The identity of bound metal in QueD expressed by the native organism living in natural circumstances is as of yet unknown. But the tendency of over expressed enzymes grown in LB media to incorporate Fe preferentially has been shown (36), which explains the initial reports that BsQueD is an iron-containing enzyme. Growing the host bacterium in minimal media and supplementing with a desired metal has been effective for incorporating Mn and Co, but difficulties have been encountered for the incorporation of Cu because the Cu precipitates out of the phosphate buffer. A study has been conducted that suggests that the location of protein folding dictates the identity of incorporated metal (37). Proteins that fold in the cytoplasm of a cell contain Mn; while proteins that are exported to the

periplasm before folding contain Cu. This may not be relevant in gram-positive *B. subtilis*. However, *E. coli* does have a periplasmic space, and therefore, expression of BsQueD in the host cell might influence the metal incorporation differently than for BsQueD expressed in the native organism. Interestingly, AQueD is a secreted enzyme, and it incorporates Cu when grown in its native organism (38). More *in vivo* and *in vitro* metal incorporation studies should be conducted to better understand how the identity of the bound metal affects its incorporation and enzyme efficiency.

While no mutagenic studies have been able to conclusively confirm that one metal-binding site is more crucial for catalysis, structural studies of both OxDC and BsQueD (39, 22) have revealed a loop region at the N-terminal domain that may be acting as a lid over the catalytic channel. It has been argued that this structural feature is evidence that the reaction is happening primarily at the N-terminal domain, and the C-terminal domain may be contributing only slightly or not at all to the activity of the enzyme. Further mutagenesis of the glutamate residues as described above should be conducted to determine if activity is indeed carried out primarily (or exclusively) in the N-terminal domain.

REFERENCES

22. Gopal, B., Madan, L. L., Betz, S. F., and Kossiakoff, A. A. (2005) The crystal structure of a quercetin 2,3-dioxygenase from *Bacillus subtilis* suggests modulation of enzyme activity by a change in the metal ion at the active site(s). *Biochemistry 44*, 193-201.

23. Steiner, R. A., Kalk, K. H., and Dijkstra, B. W. (2002) Anaerobic enzyme-substrate structures provide insight into the reaction mechanism of the copper-dependent quercetin 2,3-dioxygenase. *Proceedings of the National Academy of Sciences of the United States of America 99*, 16625-16630.

24. Schaab, M. R., Barney, B. M., and Francisco, W. A. (2006) Kinetic and spectroscopic studies on the quercetin 2,3-dioxygenase from Bacillus subtilis. *Biochemistry 45*, 1009-1016.

25. Dunwell, J. M., Purvis, A., and Khuri, S. (2004) Cupins: the most functionally diverse protein superfamily? *Phytochemistry 65*, 7-17.

26. Fusetti, F., Schroter, K. H., Steiner, R. A., van Noort, P. I., Pijning, T., Rozeboom, H. J., Kalk, K. H., Egmond, M. R., and Dijkstra, B. W. (2002) Crystal structure of the copper-containing quercetin 2,3-dioxygenase from *Aspergillus japonicus*. *Structure 10*, 259-268.

27. Catic, A., Sun, Z. J., Ratner, D. M., Misaghi, S., Spooner, E., Samuelson, J., Wagner, G. and Ploegh, H. L. (2007) Sequence and structure evolved separately in ribosomal ubiquitin variant. *EMBO Journal* 26, 3474-3483.

28. Ho, S. N., Hung, H. D., Horton, R. M., Pullen, J. K., and Pease, L. R. (1989) Site-directed mutagenesis by overlap extension using the polymerase chain reaction. *Gene* 77, 51-59.

29. Notredame, C., Higgins, D. G., and Heringa, J. (2000) T-Coffee: A Novel Method for Fast and Accurate Multiple Sequence Alignment. *Journal of Molecular Biology* 302, 205-217.

30. UCSF Chimera--a visualization system for exploratory research and analysis. Pettersen EF, Goddard TD, Huang

CC, Couch GS, Greenblatt DM, Meng EC, Ferrin TE. *J Comput Chem.* 2004 Oct;25(13):1605-12.

31. Esposito, D. and Chatterjee, D. K. (2006) Enhancement of soluble protein expression through the use of fusion tags. *Biotechnology* 17, 353-358.

32. Woestenenk, E. A., Hammarstrom, M., van den Berg, S., Hard, T., and Berglund, H. (2004) His tag effect on solubility of human proteins produced in *Escherichia coli*: a comparison between four expression vectors. *Journal of Structural and Functional Genomics* 5, 217-229.

33. Moomaw, E. W., Angerhofer, A., Moussatche, P., Ozarowski, A., Garcia-Rubio, I. and Richards, N. G. J. (2009) Metal Dependence of Oxalate Decarboxylase Activity. *Biochemistry* 48, 6116-6125.

34. Merkins, H., Kappl, R., Jokob, R. P., Schmid, F. X., and Fetzner, S. (2008) Quercetinase QueD of Streptomyces sp. FLA, a monocupin Dioxygenase with a Preference for Nickel and Cobalt. *Biochemistry* 47, 12185-12196.

35. Balogh-Hergovich, E. and Speier G. (2001) Kinetics and Mechanism of the Base-Catalyzed Oxygenation of Flavonol in DMSO-H_2O Solution. *Journal of Oragnic Chemistry* 66, 7974-7978.

36. Hoffman, B. J., Broadwater, J. A., Johnson, P., Harper, J., Fox, B. G., and Kenealy, W. R. (1995) Lactose fed-batch overexpression of recombinant metalloproteins in Excherichia coli BL21-(DE3)-process control yielding high levels of metal incorporated, soluble protein. *Protein Expression Purification* 6, 646-654.

37. Tottey, S., Waldron, K. J., Firbank, S. J., Reale, B., Bessant, C., Sato, K., Cheek, T. R., Gray, J., Banfield, M. J., Dennison, C., and Robinson, N. (2008) Protein-folding location can regulate manganese-binding versus copper- or zinc-binding. *Nature* 455, 1138-1142.

38. Oka, T., Simpson, F. J., Child, J. J., Mills, S. C. (1971) Degradation of rutin by Aspergillus flavus. Purification of the dioxygenase, quercetinase. *Canadian Journal of Microbiology* 17, 111-118.

39. Svedruzic, D., Liu, Y., Reinhardt, L. A., Wroclawska, E., Cleland, W. C., and Richards, N. G. J. (2007) Investigating the roles of putative active site residues in the oxalate decarboxylase from *Bacillus subtilis*. *Archives of Biochemistry and Biophysics* 464, 36-47.

Chapter 3

THE PURIFICATION PROCESS

INTRODUCTION

Traditionally, a bottleneck for enzyme research has been isolation of enzymes. Cells contain thousands of proteins (40), but generally a protein of interest constitutes only <0.1% of the total dry weight of a cell (41). To understand the behavior of a single molecule out of the soup of biological material, it is usually necessary to remove as much of the other substances as possible. There are several protein properties that can be exploited to effectively isolate a given enzyme to over 90% purity. These properties include: charge, polarity, size and binding specificity (41,42). Previously, quercetin 2,3-dixogyenase from *Bacillus subtilis* (BsQueD) was overexpressed in *E. coli* and purified by a process that utilized both its size and charge in gel filtration and ion exchange chromatography (43). Once cells were opened and cell debris was removed, the mixture was passed through an anion exchange column (DEAE sephacel), followed by salt precipitation (sodium sulfate) and finally a size exclusion column (Ultrogel AcA44.) This process took a full two days to complete.

As a general rule, the best enzyme purification schemes are the ones that are completed in the fewest steps. This is because each purification step inevitably causes some loss of product, and the more steps the enzyme must go through, the lower the final yield of enzyme collected and the more enzyme

activity is lost. In an effort to lessen the number of purification steps and shorten the amount of time required for enzyme preparation, a 6xHis tag was engineered at the N-terminus of BsQueD. The resulting enzyme (6xHis-BsQueD) could then be purified with a single column (Nickel nitriloacetic acid; Ni-NTA) in only a few hours (FIG. 3.1).

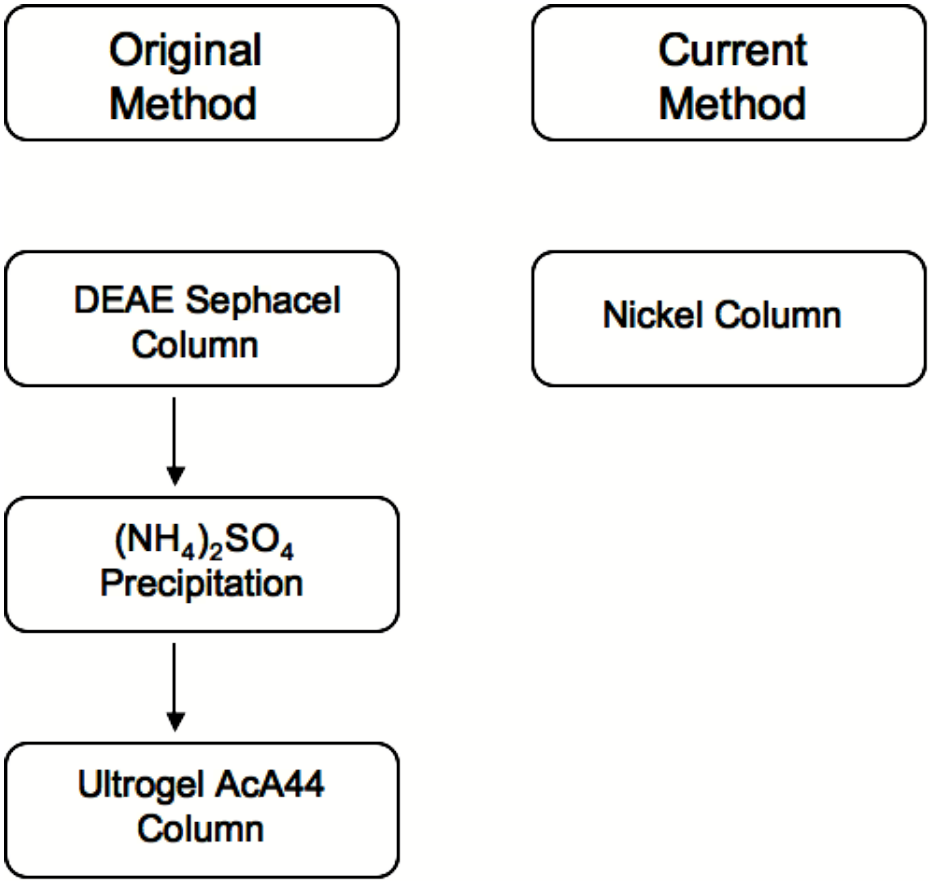

FIG. 3.1: **A comparison of the purification steps required by the former enzyme isolation method versus the current purification protocol.**

MATERIALS AND METHODS

Specific kits listed were used as directed by the manufacturer. Luria-Bertani (LB) broth was obtained from EMD. Protein concentration was measured with Quick Startô Bradford Reagent (Bio-Rad) with bovine serum albumin as a standard (Pierce). Sodium dodecyl sulfate-polyacrylamide gel electrophoresis (SDS-PAGE) was performed using equipment and reagents from Bio-Rad. The proteins were visualized with Coomassie Brilliant Blue R-250 (Bio-Rad). Plasmid purifications were done with the QIAprepÆ Spin miniprep kit (Qiagen). DNA isolations from PCR reactions and agarose gels were performed with the WizardÆ SV gel and PCR clean-up system (Promega). The parent plasmid, pQuer4, was constructed previously by Dr. Brett Barney. Phusion ® DNA polymerase was obtained from Finnzymes. Nucleotides were from a Promega dNTP mix. T4 DNA ligase was purchased from Invitrogen. All restriction enzymes are FastDigest® Enzymes from Fermentas Life Sciences. DNA was visualized on agarose gels with SYBR®Safe DNA gel stain purchased from Invitrogen. The plasmid vector, pET30a(+) was obtained from Novagen. *Escherichia coli* OneShot® TOP10, and BL21(DE3) chemically competent cells were purchased from Invitrogen. Isopropyl-1-thio-β-D –galactopyranoside (IPTG) was obtained from Gold Biotechnology, Inc. Protein isolations were performed with diethylaminoethyl (DEAE) sephacel resin (Sigma-Aldrich) and Ultrogel AcA44 resin (Sigma) or His-Bind® Fractogel® Resin purchase from Novagen and

columns purchased from Bio-Rad. All other chemicals and reagents were of the highest purity available (Sigma-Aldrich). All primers were synthesized and purified by standard desalting by Integrated DNA Technolgies (IDT).

*Original Column Purification***.** Cells were lysed with a French pressure cell at 700 psi. The lysate was then centrifuged at 20, 000x g in a Sorvall 5C Plus centrifuge for 20 min at 4 ˚C. The supernatant was filtered through a Milipore 2 μm filter and loaded at a rate of 1mL/min onto a DEAE sephacel column. The flow through was observed at 280 nm while 50 mM tris(hydroxymethyl)amino methane (Tris) pH 7.5 was passed through the column. After a peak was observed and the A_{280} returned to baseline levels, a 125 mM NaCl in Tris pH 7.5 buffer solution was passed through the column until the A_{280} peaked again and returned to baseline. Finally a 150 mM NaCl in Tris pH 7.5 buffer solution was used to elute BsQueD. Fractions that corresponded to peaks in the absorbance at 280 nm were tested for activity by the standard spectrophotometric assay. Once a peak was determined to contain BsQueD, fractions that corresponded to that peak were loaded onto a 12% sodium dodecyl sulfate polyacrylamide gel electrophoresis (SDS-PAGE) gel. The purest, most active fractions were combined, and ammonium sulfate was added slowly at 4 ˚C until the solution was 55% ammonium sulfate, which precipitates BsQueD at 4 ˚C. Precipitated BsQueD in ammonium sulfate was centrifuged at 20,000x g in a Sorvall 5C-Plus centrifuge at 4 ˚C for 20 min. The supernatant was discarded, and the pellet was

resuspended in 2 mL 200 mM NaCl, 50 mM Tris pH 7.5. The protein was then carefully loaded onto an Ultrogel AcA44 size-exclusion column. Two hundred mM NaCl, 50 mM Tris buffer pH 7.5 was passed through this column for at least 16 h. A_{280} peaks were again tested for activity and purity by photometric assays and 12% SDS-PAGE gels. The purest, most active fractions were then combined and concentrated to approximately 2 mL in a Milipore 10,000 MWCO concentrator in a Sorval swinging bucket rotor centrifuge at 4 ˚C (Figure 3.1). Protein concentration was determined by Bradford assay using BSA protein standards from Pierce.

Impurities were further characterized by trpysin digest followed by matrix assisted laser desorption/ionization time-of-flight mass spectrometry (MALDI-TOF MS). Bands were cut from a 12% SDS-PAGE gel with a razor blade, and then digested with a Calbiochem Proteo All-in-One Trypsin digest kit. Digested protein was then analyzed in the Arizona State University Protein Lab on a Voyager DE STR MALDI-TOF mass spectrometer. The online program Aldente (44) was used to analyze the peak lists.

*Engineering a 6xHis tag at the N-terminus of BsQueD***.** The overlapping extension mutagenesis technique (as described in chapter 2) was used to remove 26 bases between the coding sequence for the 6xHis tag and the beginning of the coding sequence for BsQueD in pQuer4 (FIG. 3.2 (45)). Simultaneously, these primers added the 16 nucleotide coding sequence for an enterokinase protein

cleavage site between the tag and the gene (FIG. 3.3). Two sets of primers were designed. The first set produced a front fragment that ended adjacent to the unwanted 26 base-pair sequence between the 6XHis tag and the BsQueD gene. The primer at this end (oligo 31) contained a hanging tail that encoded for the enterokinase sequence. The second pair of primers produce a fragment that begins with a hanging enterokinase sequence followed by the base pairs of quercetinase directly after the unwanted 26 bp region until the end of the gene. Two master mixtures were made: F (front segment) contained oligo 31 and Wilson 43, and B (back) contained oligo 32 and Wilson 44 (TABLE. 3.1). Both mixtures were cycled on the program JAN13 (TABLE. 3.2). A front and back mixture were each diluted one tenth and combined for the second round of PCR (FIG. 3.4). It was also cycled on program JAN13 (TABLE. 3.2).

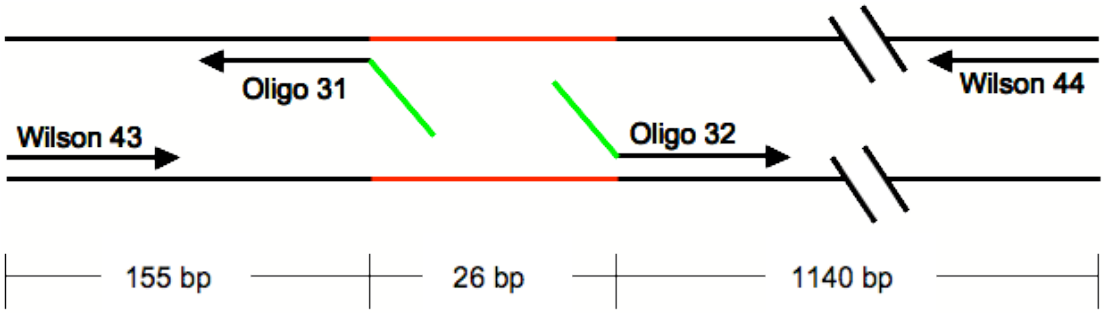

FIG. 3.2: **Overlap extension mutagenesis scheme for the addition of an N-terminal His tag**. The overlapping extension mutagenesis technique was used to eliminate 26 bases while introducing a 16 base pair sequence in their place. This was accomplished by designing primers that primed directly adjacent to the undesired region (shown on the parent strands as a red line). Bases were added by designing 5'→3' hanging tails that were reverse complements of one another (shown as green tails on the primers).

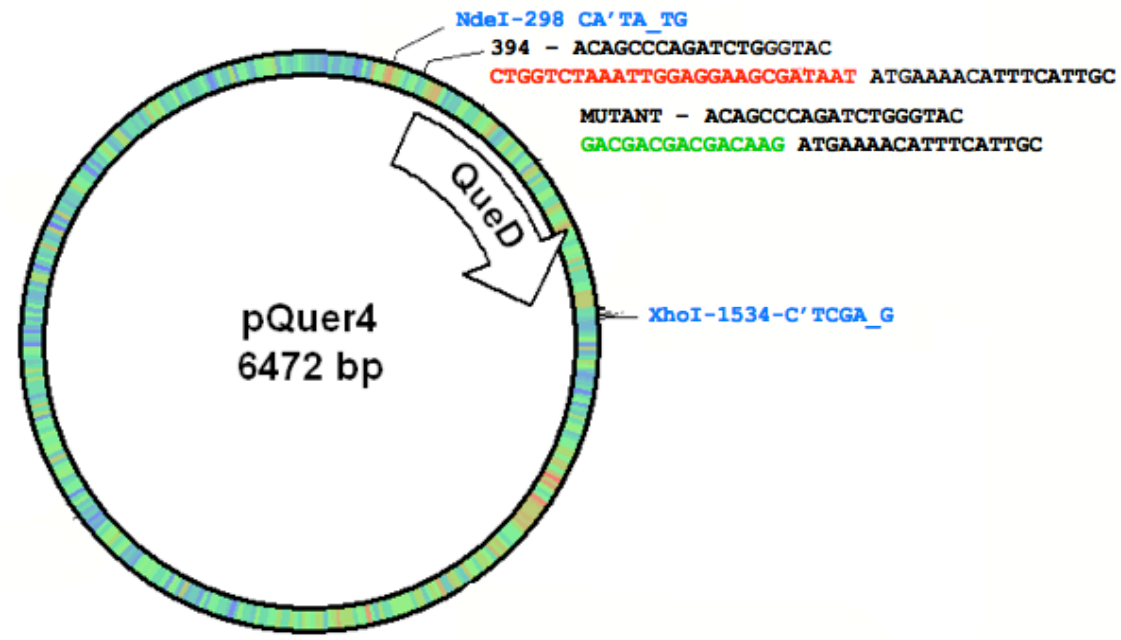

FIG. 3.3: **Plasmid map for His tag mutagenesis**. Primers were designed to create a mutated fragment at the N-terminus of the BsQueD gene between the NdeI and XhoI restriction sites. Two sequences are shown starting at base pair 394 of the wild type plasmid. The top sequence is the wild type sequence. Priming bases are shown in black, and cut out bases are shown in red. The bottom sequence is the mutant sequence. Again priming bases are shown in black, and added bases are shown in green.

TABLE. 3.1

Primers for engineering a 6xHis tag.

Oligo 31 CTT GTC GTC GTC GTC GGT ACC CAG ATC TGG GCT GT
Oligo 32 GAC GAC GAC GAC AAG ATG AAA ACA TTA TGT ACA CAT TCA TTG C
Wilson 43 GTG AGC GGA TAA CAA TTC CCC TC
Wilson 44 GCC AAC TCA GCT TCC TTT CGG G

TABLE. 3.2

PCR Program JAN13

98 ˚C	30 s	1X
98 ˚C	5 s	
72 ˚C-64 ˚C	10	25X
72 ˚C	15 s	
72 ˚C	5 min	1X

The final fragment was digested by NdeI (upstream of the gene) and XhoI (downstream of the gene) for 1 h at 37 ˚C. The fragment was then ligated in digested pET30a(+) vector overnight at 16 ˚C. *E. coli* chemically competent OneShot® TOP10 cells were transformed by heat shock with the construct for storage. Cells were incubated for 30 min on ice with newly ligated plasmid DNA. Cells were then heat shocked at 42 ˚C for 45 s, and then they were incubated on ice for 2 min. One half mL of warmed LB broth was added to the cells, and then a recovery incubation was conducted for 1 h at 37 ˚C and shaking at 200 rpm. One

hundred to 150 μL of recovery broth was plated on kanamycin-LB/Agar plates (3% kanamycin). The transformants were incubated overnight at 37 ˚C. Well-formed, distinct colonies were selected and incubated overnight in kanamycin-LB. Turbid overnights were harvested for plasmid purification, and DNA was analyzed by digestion and agarose gel electrophoresis followed by DNA sequencing in the DNA lab at Arizona State University. Chemically competent *E. coli* BL21(DE3) cells were then transformed by heat shock with plasmid purified with a Qiagen kit from the storage cell line.

Expression was confirmed by inoculating two 1 L M9 minimal media culture flasks with overnights of *E. coli* that overexpress the mutant. After both cultures reached an OD_{600} of 0.6-0.9, 1 mL of 1 M $MnCl_2$ was added to both and IPTG was added to the sample culture. No IPTG was added to the control culture. Induced and control cultures were incubated for 4 h at 20 ˚C with shaking at 200 rpm. Cultures were harvested after 4 h by centrifuging at 20, 000 x g. Cell pellets were stored at -80 ˚C until they were opened using a French pressure cell at 700 psi. The lysed cells were then centrifuged at 20,000 x g. A sample of supernatant from both the induced and control cultures were examined on a 12% SDS-PAGE gel.

Nickel Column Purification. Cells were lysed and centrifuged as before. However, the supernatant was then loaded onto Novagen's HisBind Fractogel resin charged with nickel ions in a Bio-Rad glass column. The column was washed

with ten times bed volume of binding buffer (300 mM NaCl, 50 mM NaH_2PO_4, 10 mM imidazole pH 8.00). The column was again washed with six times bed volume of wash buffer (300 mM NaCl, 50 mM NaH_2PO_4, 20 mM imidazole pH 8.00). Enzyme was eluted with six times bed volume of elution buffer (300 mM NaCl, 50 mM NaH_2PO_4, 150 mM imidazole). Fractions were collected approximately every 500 µL per mL of resin. Fractions were then analyzed for purity by 12% SDS PAGE gel. The purest fractions were combined and concentrated in a Milipore 10, 000 MWCO concentrator as previously described (FIG. 3.1).

CD Spectroscopy. Before analysis by circular dichroism (CD) spectroscopy, it was necessary to remove all traces of Tris from the samples. This was done by centrifuging the samples at 3.0 rpm in the IEC Centra CL2 swinging bucket rotor centrifuge in a 10,000 MWCO concentrator and then adding 10% glycerol in 50 mM phospate buffer pH 8.00. The buffer exchange was performed a minimum of three times. Protein concentration was determined by Bradford assay and A_{280}. Samples were diluted to between 0.1 and 0.4 mg/ mL. Samples were analyzed in a Jasco J-1710 spectropolarimeter.

Standard Spectrophotometric Assay. The standard spectrophotometric assay was carried out in a 1 cm pathlength quartz cuvette in a Hewlett Packard 8453 UV-Visible Spectrophotometer. Fifty µL of 1.0 mM quercetin (dissolved in dimethyl sulfoxie) were mixed with 950 µL buffer a single time with a stir stick,

and the solution was blanked. To begin the assay, 5 μL of enzyme solution was added to the buffer/substrate and mixed a single time. The absorbance at 380 nm was observed for at least 60 s.

RESULTS

The SDS-PAGE gels of enzyme purified by the multiple-column method have to most prominent bands visible: one at approximately 37 kDa and the other at approximately 60 kDa. These bands were trypsin digested and their fingerprints were analyzed by MALDI-TOF MS and the database Aldente (44). The 37 kDa, as expected, is BsQueD (FIG. 3.4.) Its Aldente score is 37.33 and has 56% coverage. The next closest match, glutamine amidotransferase subunit pdxT from *Bacillus cereus*, has an Aldente score of 3.18. The higher molecular weight impurity is Elongation factor G from *E. coli* (FIG. 3.5). The aldente score for this is 68.28, and the next closest score is 19.63 for the protein alanyl-tRNA synthetase from the organism *Bartonella tribocorum*.

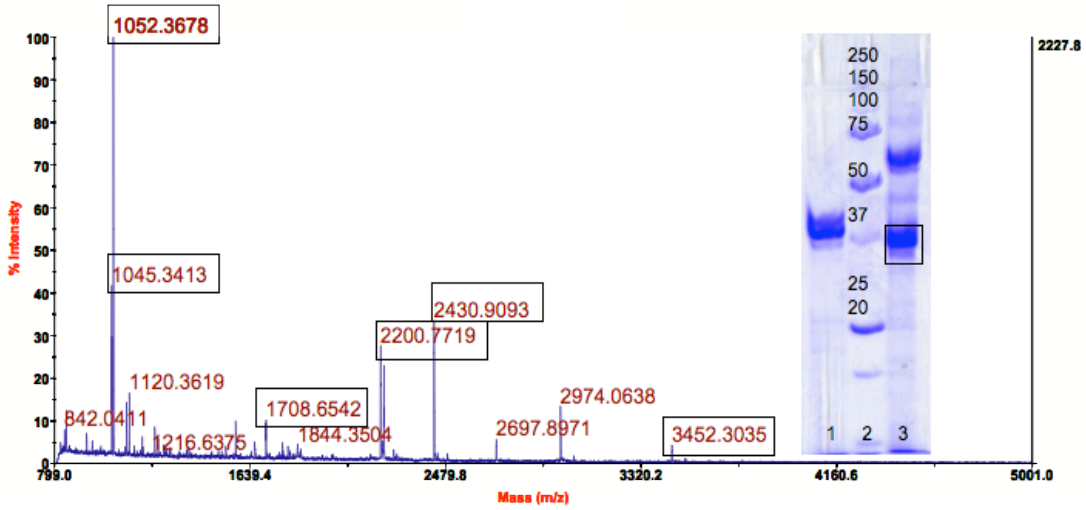

FIG. 3.4: **The MALDI MS spectrum of a 37 kDa band (boxed) purified from a PAGE gel and digested with trypsin**. Peaks highlighted by boxes correspond to trypsin-digested peaks of BsQueD according to the mass fingerprinting software Aldente available on expasy.org.

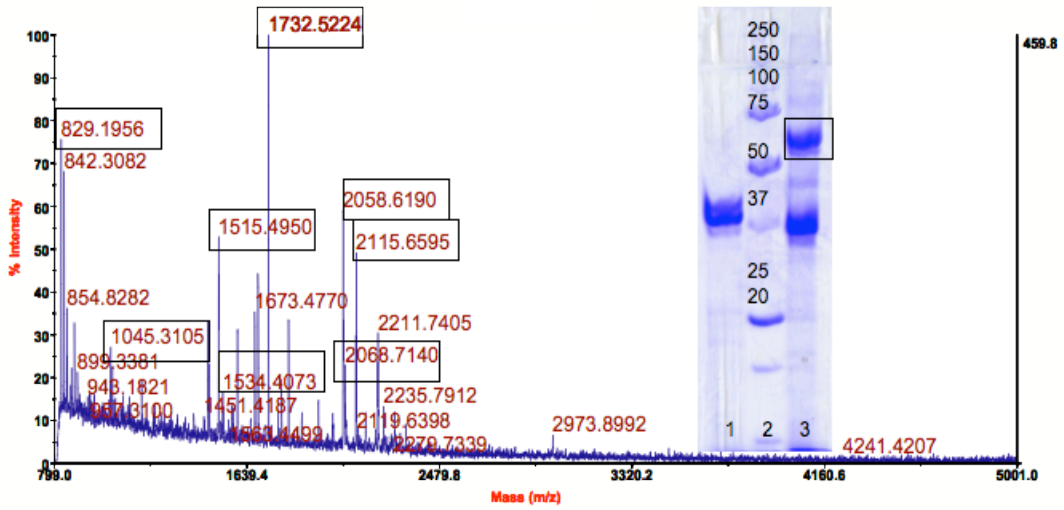

FIG. 3.5: **The MALDI MS spectrum of a 60 kDa band (boxed) purified from a PAGE gel and digested with trypsin**. Peaks highlighted by boxes correspond to trypsin-digested peaks of Elongation factor G from *E. coli* according to the mass fingerprinting software Aldente available on expasy.org.

The overlapping extension mutagenesis technique was successfully used to engineer a 6xHis tag onto BsQueD (6xHis-BsQueD.) The successful PCR was confirmed by 1% agarose gel electrophoresis (FIG. 3.6). All of the annealing temperatures produced both a front fragment that was about 200 bp in size and a back fragment that was about 1200 bp in size. In the second round of PCR, temperatures 64˚C to 69˚C successfully produced a full length fragment by annealing and elongating the front and back fragments (FIG. 3.7). After transformation into *E. coli* DH5α chemically competent cells, digestion and ligation into pET30a(+) were also confirmed by 1% agarose gel electrophoresis

with positive (pQuer4) and negative (pET30a(+)) controls. After plasmids were purified from the transformant colonies, they were digested with XhoI and NdeI for analysis. A positive control plasmid (pQuer4) and a negative control plasmid (pET30a(+)) were also digested with XhoI and NdeI. All the lanes containing transformant plasmids had two bands that migrated the same distance as two bands in the positive control lane (FIG. 3.8). This was then followed by sequencing in the DNA laboratory at Arizona State University with primers Wilson 43 and Wilson 44 as sequencing primers.

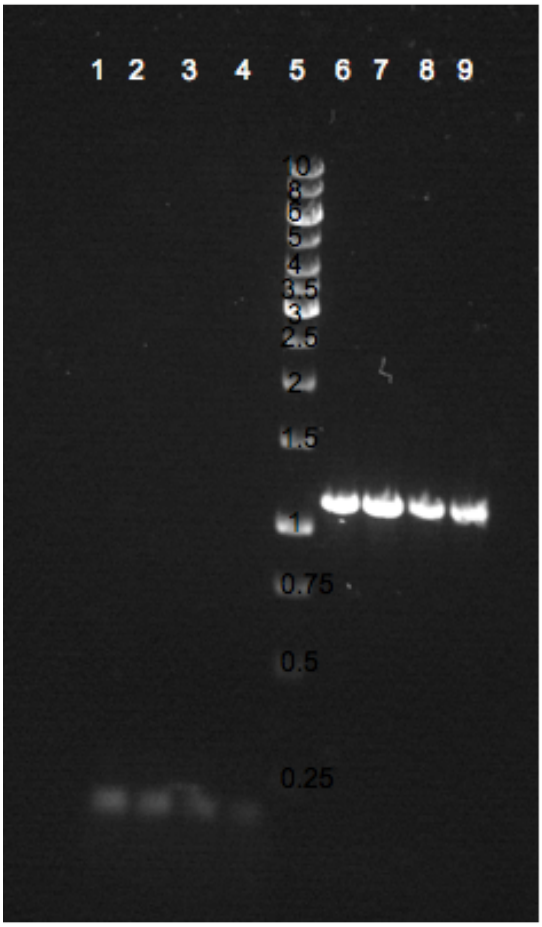

FIG. 3.6: **First round of mutagenic PCR**. The overlapping extension mutagenesis technique requires two rounds of PCR to introduce the intended mutations. After each round of PCR gel electrophoresis was performed on a 1% agarose gel to confirm elongation. The first round of PCR at several annealing temperatures produces a front and back fragment. Lanes 1-4 are back fragments Lane 1: 64.0 ˚C; Lane 2: 65.7 ˚C; Lane 3: 69.0 ˚C; Lane 4: 70.5 ˚C; Lane 5: Fermentas GeneRulerô 1 kb DNA ladder, 5 µL. Sizes of DNA standards are labeled and reported in Kb; Lanes 5-8 are front fragments Lane 6: 64.6 ˚C; Lane 7: 67.2 ˚C; Lane 8: 72.0 ˚C.

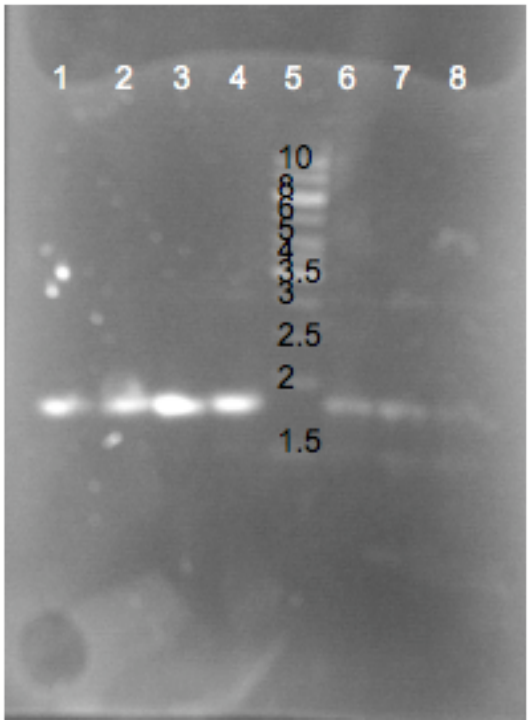

FIG. 3.7: **Second round of mutagenic PCR**. In the second round of PCR, the front and back segments are overlapped to produce a full length, mutated fragment. This was also performed at several annealing temperatures. Lane 1: 64.6 ˚C; Lane 2: 65.7 ˚C; Lane 3: 67.2 ˚C; Lane 4: 69.0 ˚C; Lane 5 Fermentas GeneRulerô 1 kb DNA ladder, 5 µL. Sizes of DNA standards are labeled and reported in Kb; Lane 6: 70.5 ˚C; Lane 7: 71.5 ˚C; Lane 8: 72.0 ˚C.

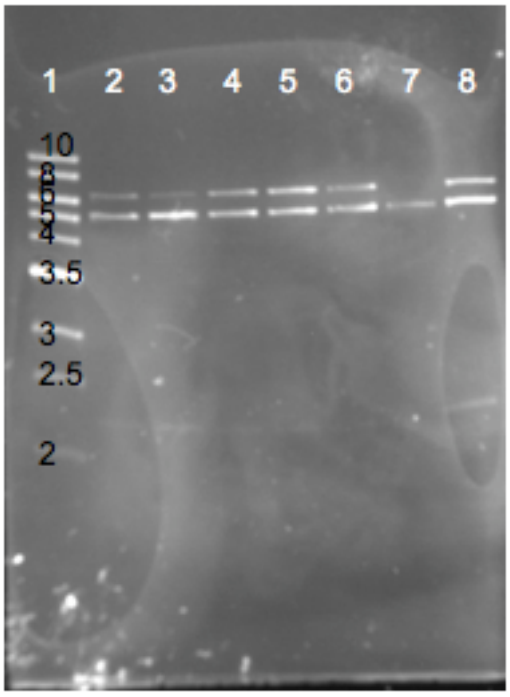

FIG. 3.8: **Ligation confirmation**. The successful ligation and transformation of the 6xHis Tag fragment into the vector pET30a(+) was confirmed by digestion and 1% agarose gel electrophoresis. Lane 1: Fermentas GeneRulerô 1 kb DNA ladder, 5 µL. Sizes of DNA standards are labeled and reported in Kb; Lanes 2-6: BamHI and KpnI digested His-wt plasmids from single colonies of *E. coli* OneShot® TOP10 chemically competent cells Lane 7: negative control, pET30a(+); Lane 8: positive control, BamHI and KpnI digested pQuer4.

After DNA sequencing confirmed the in-frame fusion of a 6XHis tag with an enterokinase cleavage linker with the BsQueD gene, an expression test was conducted to ensure that the fused enzyme was expressing and that it was soluble. Figure 3.9 is a 12% SDS-PAGE gel of the supernatant of the lysates from induced and control (non-induced) cultures. At approximately 39 kDa, a distinct expression band is clearly visible in the induced lane that is not present in the control lane.

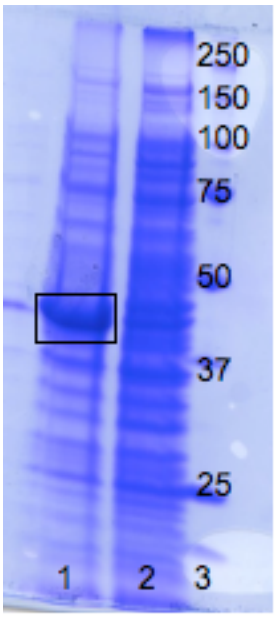

FIG. 3.9: **Protein expression confirmation**. Protein expression was confirmed by growing *E. coli* BL21(DE3) under inducing and control (non inducing) conditions. Lane 1: cell lysate of culture induced with 50 mg IPTG/ L of medium; Lane 2: cell lysate from control (non-induced) culture Lane 3: BioRad Precision Plus Proteinô standard ladder, 15 µL. Sizes of the protein standards in lane 1 are labeled and reported in kDa.

The purity of a sample of enzyme isolated with a nickel column was compared to a sample of enzyme purified by the previous method on a 12% SDS-PAGE gel (FIG. 3.10). Enzyme was visualized by staining with Coomassie blue. Purity was compared with a Kodak System. The multi-column sample was 96% pure, and the nickel column purified sample was 99% pure.

.

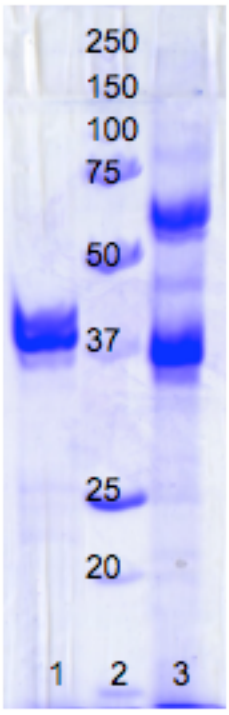

FIG. 3.10: **12% SDS-PAGE gel comparing purity of enzyme**. Lane 1: protein engineered with a 6xHis tag purified with a nickel column; Lane 2: Biorad Precision Plus Proteinô standard ladder, 15 µL. Sizes of the protein standards in lane 1 are labeled and reported in kDa; Lane 3: Wild type protein purified by the former method.

The primary protein sequence of the calculated from the plasmid sequence and is shown in FIG. 3.11.

MHHHHHHSSG LVPRGSGMKE TAAAKFERNH MDSPDLGTDD

DDDKMKTLCT HSLPKEKMPY LLRSGEGERY LFGRQVATVM

ANGRSTGDLF EIVLLSGGKG DAFPLHVHKD THEGILVLDG

KLELTLDGER YLLISGDYAN IPAGTPHSYR MQSHRTRLVS

YTMKGNVAHL YSVIGNPYDH AEHPPYASEE VSNERFAEAA

AVATIVFLDE AKPACSAKLA ELTELPDGAV PYVLESGEGD

RLLTGDQLHR IVAAQKNTDG QFIVVSSEGP KGDRIVDHYH

EYHTETFYCL EGQMTMWTDG QEIQLNPGDF LHVPANTVHS

YRLDSHYTKM VGVLVPGLFE PFFRTLGDPY EGHIFPCKPQ

ALRFDRILQN IEALDLKVMK P

FIG. 3.11: **The primary sequence of 6xHis-BsQueD**. Residues shown in red are the 6xHis tag. Residues shown in blue are the linker sequence from the pET30(+)a vector. Residues shown in green are the enterokinase cleavage site, and residues shown in black are BsQueD.

A structural 3.comparison of tagged and untagged enzyme was conducted by CD spectroscopy (FIG. 3.12.) Both enzymes produce CD spectra typical of proteins that are predominately composed of β-sheets (46). In fact, wild type enzyme is 39% β-sheet and only 8% α-helix (47). An arbitrary length of wavelengths (210 to 230 nm) was compared, and it was found that the 6xHis-BsQueD signal is 85% of the untagged enzyme. Several wavelengths were directly compared to ensure that the difference in spectra was only a shift rather than a change in shape (TABLE. 3.3.)

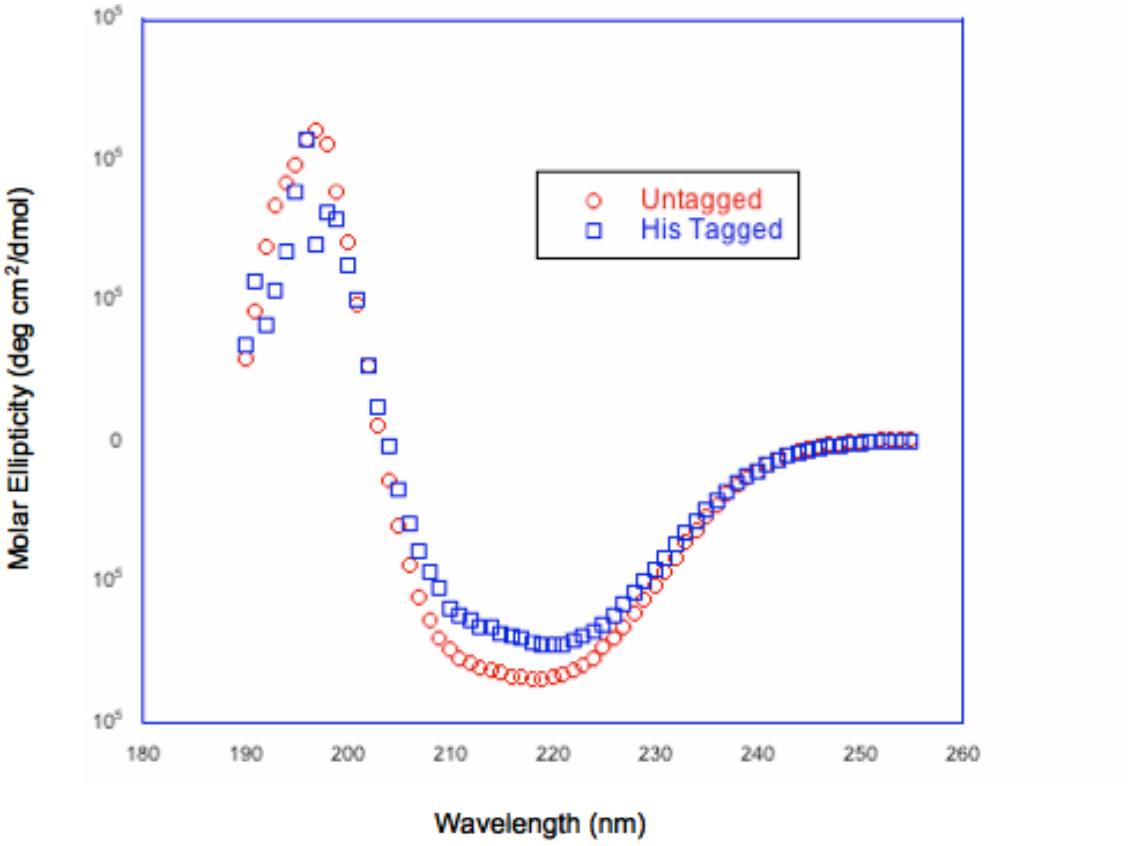

FIG. 3.12: **A comparison of the CD spectra of untagged BsQueD (red circles) and 6xHis-BsQueD (blue squares).** Both enzymes show a negative peak at approximately 218 nm and a positive peak at 196 nm, which is characteristic of β-sheet proteins. The signal of 6xHis-BsQueD is 85% of the untagged BsQueD signal.

TABLE. 3.3

Comparison of the CD spectra of BsQueD and 6xHis-BsQueD.

Wavelength (nm)	BsQueD (deg cm^2/dmol)	6xHis-BsQueD (deg cm^2/dmol)	BsQueD/6xHis-BsQueD (deg cm^2/dmol)
230	-102678	-91234.5	1.91984
225	-147122	-129432	1.93902
220	-167906	-145131	1.97357
215	-164903	-135904	2.06988
210	-148779	-118765	2.13698

A kinetic comparison of BsQueD and 6xHis-BsQueD was also conducted. The Michaelis-Menten plots are shown in FIG. 3.13.

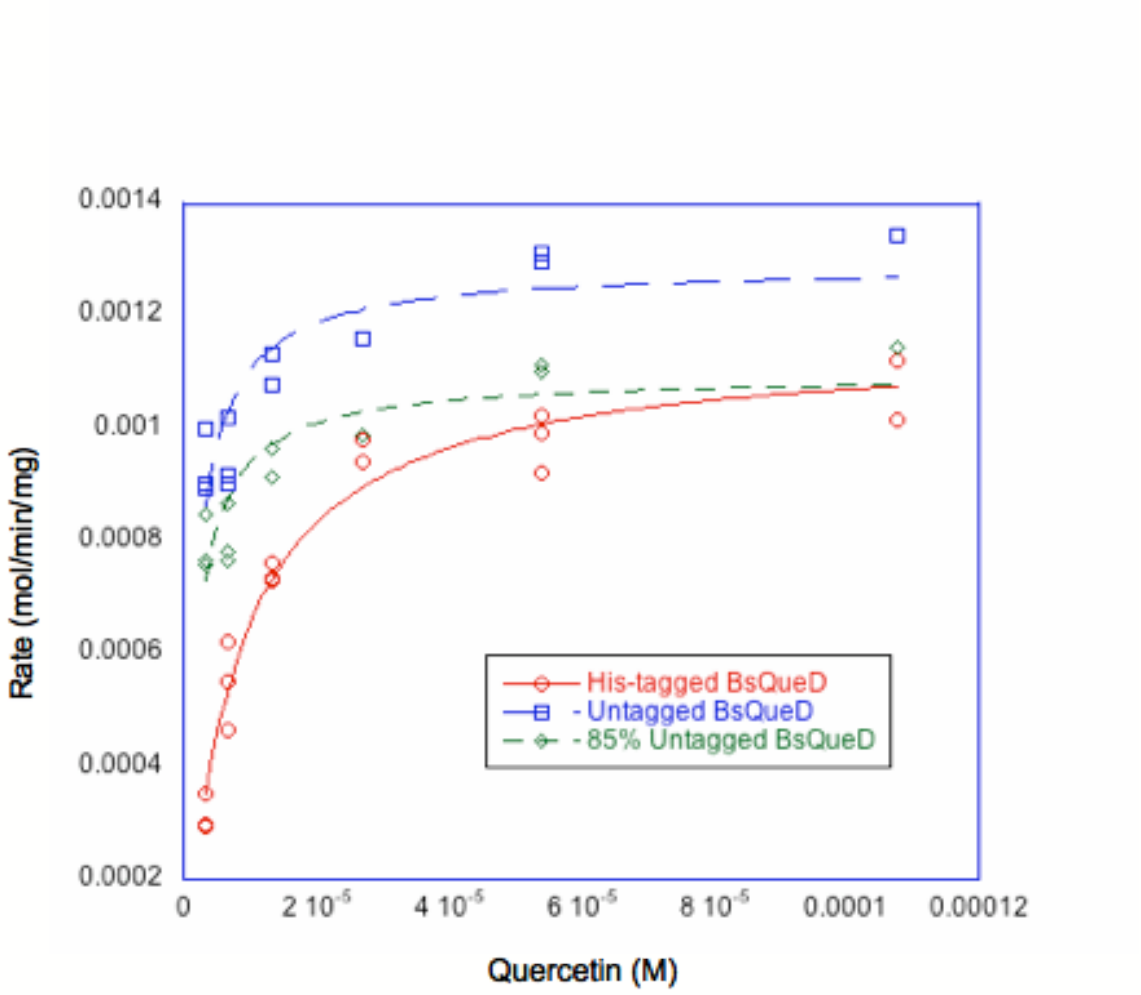

FIG. 3.13: **A comparison of kinetic parameters of untagged BsQueD and 6xHis-BsQueD**. During the initial analysis untagged BsQueD (blue squares) and 6xHis-BsQueD seem to have different K_m and V_{max}. But after CD analysis and a correction for the 85% difference in expected concentration, The V_{max} of the two enzymes are comparable, but the K_m are still slightly different (TABLE. 3.4).

TABLE. 3.4

Comparison of the kinetic parameters of BsQueD and 6xHis-BsQueD

Sample	K_m (M)	V_{max} (mol/min/mg)
Untagged BsQueD	$1.67x10^{-6}\pm3.45x10^{-7}$	$1.29x10^{-3}\pm4.51x10^{-5}$
6xHis-BsQueD	$7.68x10^{-6}\pm7.88x10^{-7}$	$1.15x10\text{-}^{3}\pm3.31x10^{-5}$
85% Untagged BsQueD	$1.67x10^{-6}\pm3.43x10^{-7}$	$1.09x10^{-3}\pm3.82x10^{-5}$

Engineering the N-terminal histidine tag onto BsQueD markedly decreased the enzyme's solubility. Untagged BsQueD can be consistently concentrated to up to 30 mg/mL pure enzyme for structural studies, such as electron paramagnetic resonance (EPR) spectroscopy. However, after several rounds of concentration, 6xHis-BsQueD remained much less concentrated (TABLE. 3.5).

TABLE. 3.5

Solubility of 6xHis-BsQueD after five rounds of concentration at pH 8.0.

Round	Concentration (mg/mL)
1	1.3
2	1.3
3	1.3
4	1.6
5	1.8

The metal content of 6xHis-BsQueD was compared to that of the untagged enzyme by ICP MS (TABLE 3.6). In an attempt to chelate the exogenous nickel, samples were rinsed through an additional column containing chelex-100 resin. Each sample was only passed over the column a single time, but this decreased the amount of nickel by an average of 37%.

TABLE. 3.6

Nickel content of BsQueD compared to 6Hix-BsQueD

Sample	Ni (M)/ Enzyme (M)
Untagged BsQueD	No Ni over detection limit
6xHis-BsQueD	2.0

DISCUSSION

Once it was decided that the purification of BsQueD by the previous, multi-column method was possibly too long for efficient production of BsQueD, the 6xHis tag and nickel column purification was an obvious choice for affinity purification. Nickel column purification has several advantages including its low metabolic cost in *E. coli* and its economically priced resin, nickel-nitrilotriacetic acid (Ni-NTA) 40) Additionally, Ni-NTA is stable through several rounds of regeneration, and the buffer conditions during a nickel column purification are relatively mild (41) One of the most compelling reasons for selecting this

particular tag was the ease of genetic engineering. The pQuer4 plasmid, created by Dr. Brett Barney, was produced with the BsQueD gene and the vector plasmid pET30a(+), which has an N-terminal poly-his tag. Dr. Barney, however, introduced the BsQueD out-of-frame from the 6xhis tag to lessen the possibility that the tag would bind extraneous transition metals, which could interfere with the quantitative metal analysis of the metalloenzyme. To redesign the enzyme fused with the 6xHis tag, it was only necessary to excise a few base pairs and realign the frame of the enzyme. This was accomplished in a single round of overlapping extension mutagenesis.

The engineering of 6xHis tag greatly reduced the amount of time required for sample preparation; less than three hours are required from the time cell pellets are opened by french pressure cell to the time enzyme samples are collected in final fractions. By contrast, 24 full hours are necessary to complete this phase of the previous, multi-column isolation method. Additionally, the 99% purity of samples prepared by nickel column purification is slightly higher than that of samples isolated by the previous method, but the 96% purity achieved by the previous method is certainly acceptable.

A structural and functional comparison of BsQueD with 6xHis-BsQueD reveals that the two enzymes are comparable. They produce very similar CD spectra consistent with the large portion of β-sheet character of the enzymes. Kinetic analysis of the tagged enzyme also produces evidence that 6xHis-BsQueD

is behaving similarly to its untagged counterpart ($V_{max6xHis\text{-}BsQueD}$=1.15x10-^{3}±3.31x10^{-5} mol/min/mg $V_{maxBsQueD}$ = 1.09x10^{-3}±3.82x10^{-5} mol/min/mg.)

6xHis-BsQueD has one obvious disadvantage, however. While it appears to be comparable structurally, it is not nearly as soluble as the untagged enzyme. BsQueD can easily be concentrated to up to 30 mg/mL, 6xHis-BsQueD can only remain soluble at up to approximately 1.5 mg/mL. This concentration is much too low for structural studies, such as electron paramagnetic resonance (EPR) spectroscopy, which requires up to 20 mg/mL enzyme to observe any signal (personal correspondance with Ravi Kumar). Several fusion tags, such as maltose binding protein and N-utilization substance A, have been shown to increase protein solubility (48) Hexahistidine, however, does not tend to increase the solubility. In fact, this particular tag has been shown to have a consistently negative impact on protein solubility (49).

In conclusion, the newly developed nickel column purification is much more efficient for producing enzyme destined for analysis that requires lower concentrations of enzyme. Kinetic analysis, CD spectroscopy, MALDI-TOF MS, and metal analysis, such as inductively coupled plasma mass spectrometry (ICP-MS) all require concentrations well under the obtainable 1.5 mg/mL of enzyme. In such cases 6xHis-BsQueD may be an efficient choice for expression and purification. However, other analyses such as EPR spectroscopy and X-ray crystallography cannot be performed with 6xHis-BsQueD because the

concentration requirements are too high (20 mg/mL and 8 mg/mL respectively (Personal Correspondence with Dr. Ravi Kumar, 50)). In these instances, the multi-step purification must be performed even though it is more time-consuming.

REFERENCES

40. Garret, R. H., and Grisham, C. M. (2005) *Biochemistry 3rd Ed.* Brooks/Cole, Belmont, p 112.

41. Voet, D., Voet, J. G., and Pratt, C. W. (2002) *Fundamentals of Biochemistry Upgrade Ed.* John Wiley & Sons, Inc, United States of America, pp 96-99.

42. Matthews, C. K., van Holde, K. E., and Ahern, K. G. (2000) *Biochemistry 3rd Ed.* Addison Wesley Longman, San Francisco, p 148.

43. Barney, B. M., Schaab, M. R., LoBrutto, R., and Francisco, W. A. (2004) Evidence for a new metal in a known active site: purification and characterization of an iron-containing quercetin 2,3-dioxygenase from *Bacillus subtilis*. *Protein Expression and Purification 35*, 131-141.

44. Gasteiger E, Hoogland C, Gattiker A, Duvaud S, Wilkins M R, Appel R D, Bairoch A, *Protein Identification and Analysis Tools on the ExPASy Server*, (In) *John M. Walker (ed): The Proteomics Protocols Handook* (2005) Humana Press, pp 571-607. http://www.expasy.org/tools/aldente/

45. Ho, S. N., Hung, H. D., Horton, R. M., Pullen, J. K., and Pease, L. R. (1989) Site-directed mutagenesis by overlap extension using the polymerase chain reaction. *Gene* 77, 51-59.

46. Greenfield, N. J. (2007) Using circular dichroism spectra to estimate protein secondary structure. *Nature Protocols* 1, 2876-2890.

47. Kabsch W., Sander C. (1983) Dictionary of protein secondary structure: pattern recognition of hydrogen-bonded and geometrical features. *Biopolymers*

48. Esposito, D. and Chatterjee, D. K. (2006) Enhancement of soluble protein expression through the use of fusion tags. *Biotechnology* 17, 353-358.

49. Woestenenk, E. A., Hammarstrom, M., van den Berg, S., Hard, T., and Berglund, H. (2004) His tag effect on solubility of human proteins produced in *Escherichia coli*: a comparison between four expression vectors. *Journal of Structural and Functional Genomics* 5, 217-229.

50. Gopal, B., Madan, L. L., Betz, S. F., and Kossiakoff, A. A. (2005) The crystal structure of a quercetin 2,3-dioxygenase from *Bacillus subtilis* suggests modulation of enzyme activity by a change in the metal ion at the active site(s).

Chapter 4

FURTHER CHARACTERIZATION

INTRODUCTION

Over the course of the mutagenic study of quercetin 2,3-dioxygenase from *Bacillus subtilis* (BsQueD) several characterization studies of the enzyme have been carried out including: stability studies and inhibition studies.

MATERIALS AND METHODS

Buffers were purchased from Sigma Aldrich. Flavone compounds were purchased from Indofine Chemical Inc. All enzyme samples were purified by the original method section 3.2.1 in chapter 3. Protein concentration was measured with Quick Start ô Bradford Reagent (Bio-Rad) with bovine serum albumin as a standard (Pierce).

*Standard Spectrophotometric Assay***.** The standard spectrophotometric assay is carried out in a 1 cm pathlength quartz cuvette in a Hewlett Packard 8453 UV-Visible Spectrophotometer. Fifty µL of 1.0 mM quercetin (dissolved in dimethyl sulfoxide) were mixed with 950 µL buffer a single time with a stir stick, and the solution was blanked. To begin the assay, 5 µL of enzyme solution was added to the buffer/substrate and mixed a single time. The absorbance at 380 nm was observed for at least 60 s.

For inhibition studies, 25 µL of quercetin (dissolved in dimethyl sulfoxide) were added at the same time as 25 µL of inhibitor (dissolved in dimethyl

sulfoxide). Stock quercetin concentrations ranged between 2.2 mM and 0.14 mM. Stock concentrations of kojic acid were 100 mM. Stock concentrations of 3,7-dihydroxyflavone were 2.2 mM, and stock concentrations of 3,7,3'-trihydroxyflavone were 2.2 mM and 1.1 mM.

RESULTS

The activity of BsQueD was monitored several times over an eighteen-day period. Samples stored at -20˚C (FIG. 4.1) retained much more activity than samples stored at 4˚C (FIG. 4.2), which is evident by comparing sample 1 (0 mM NaCl, 0% glycerol) from each trial. The samples stored at 4˚C retained only 2% of their activity compared to 49% of activity that the frozen samples retained. After 18 days and three freeze/thaw cycles, samples containing 20% glycerol retained almost all their total activity.

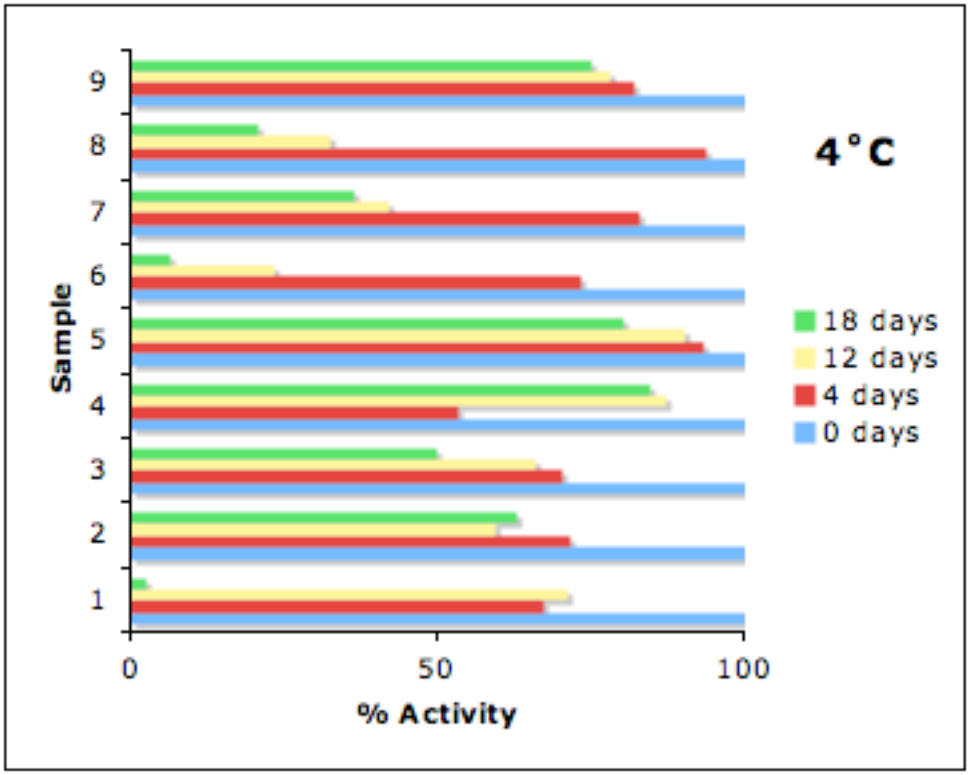

FIG. 4.1: **Samples of BsQueD were stored at 4 ˚C, and their activities were monitored over an eighteen-day period**. The composition of each sample is as follows: 1 0 mM NaCl, 0% glycerol. 2: 50 mM NaCl, 10% glycerol. 3: 100 mM NaCl, 10% glycerol. 4: 50 mM NaCl, 20% glycerol. 5: 100 mM NaCl 20% glycerol. 6: 50 mM NaCl, 0% glycerol. 7: 100 mM NaCl, 0% glycerol. 8: 0 mM NaCl, 10% glycerol. 9: 0 mM NaCl, 20% glycerol.

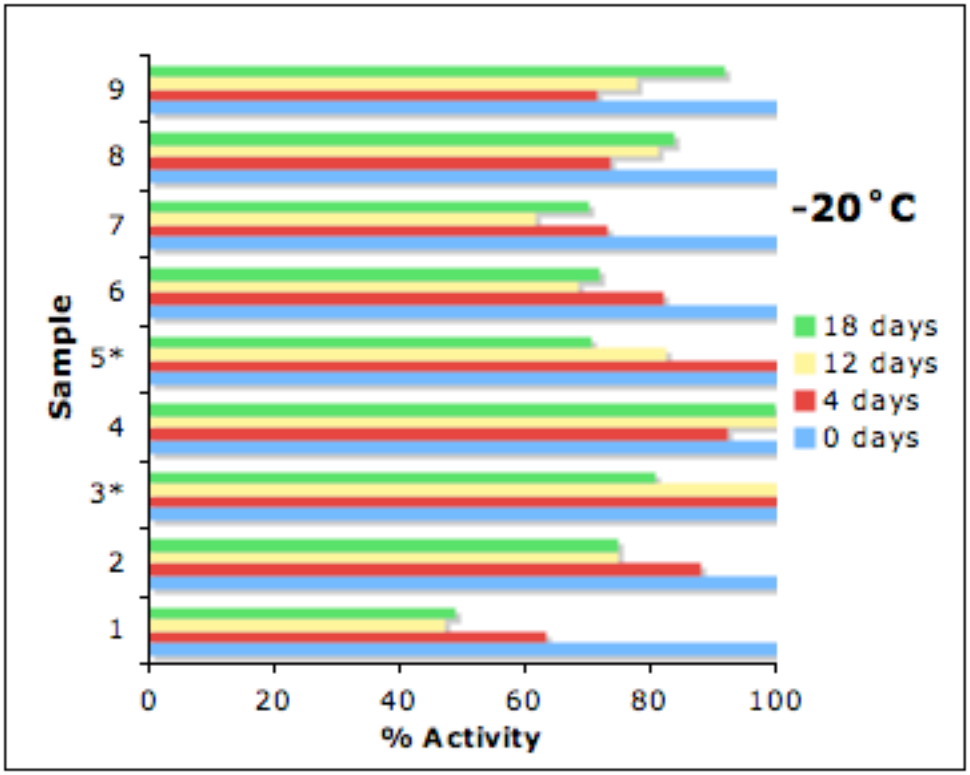

FIG. 4.2: **Samples of BsQueD were stored at -20 ˚C, and their activities were monitored over an eighteen-day period**. The composition of each sample is as follows: 1 0 mM NaCl, 0% glycerol. 2: 50 mM NaCl, 10% glycerol. 3: 100 mM NaCl, 10% glycerol. 4: 50 mM NaCl, 20% glycerol. 5: 100 mM NaCl 20% glycerol. 6: 50 mM NaCl, 0% glycerol. 7: 100 mM NaCl, 0% glycerol. 8: 0 mM NaCl, 10% glycerol. 9: 0 mM NaCl, 20% glycerol. *Samples were first recorded to have a higher activity than the average activity.

Inhibition studies of BsQueD were also conducted starting with kojic acid (KA) FIG. 4.3). KA appears to behave as a non-competitive inhibitor in the quercetinase catalytic reaction. The enzymatic parameters are displayed in TABLE. 4.1.

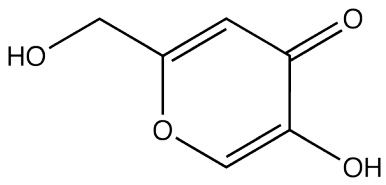

FIG. 4.3: **The chemical structure of kojic acid**.

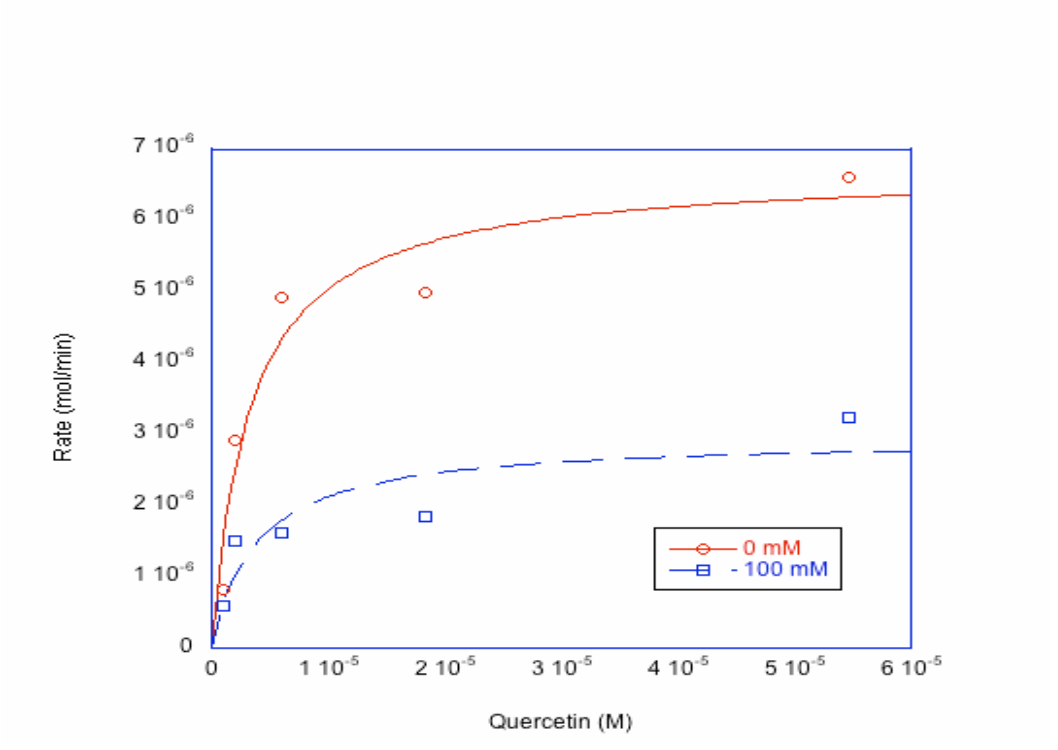

FIG. **4.4: KA seems to behave as a non-competitive inhibitor of BsQueD**.

The red, solid line is 0 mM KA, and the blue, dashed line is 100 mM KA.

TABLE. 4.1

Kinetic parameters of the inhibition of BsQueD by kojic acid.

	K_m (M)	V_{max} (mol/min/mg)
0 mM kojic acid	$3.74x10^{-6}$±$8.42x10^{-7}$	$6.95x10^{-6}$±$3.75x10^{-7}$
100 mM kojic acid	$3.47x10^{-6}$±$1.88x10^{-7}$	2.92x10-6±$4.12x10^{-7}$
K_i (M)	$1.80x10^{-3}$	

Another inhibitor was found, 3,7,3'-trihydroxyflavone ((373p) FIG. 4.5). This inhibitor behaves exactly like a competitive inhibitor at pH 8.0 (FIG. 4.7), but at pH 7.5 (FIG. 4.6) and pH 8.5 (FIG. 4.8), it seems to be behaving in a more complicated way.

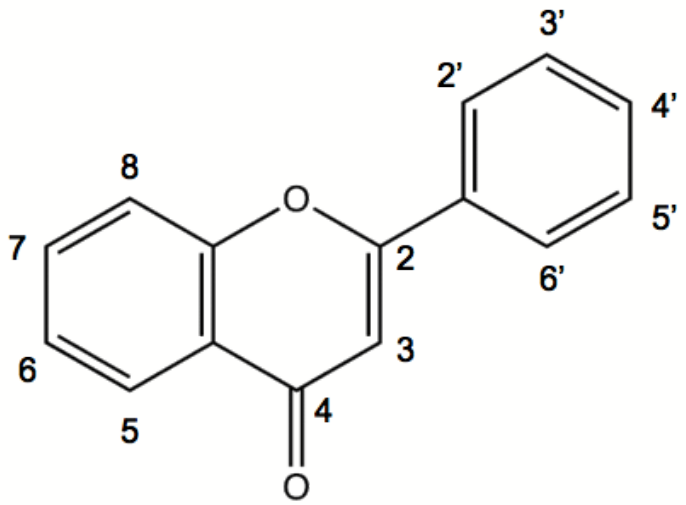

FIG. 4.5: **The inhibitor 373p is substituted at the 3, 7, and 3' carbons of flavone**.

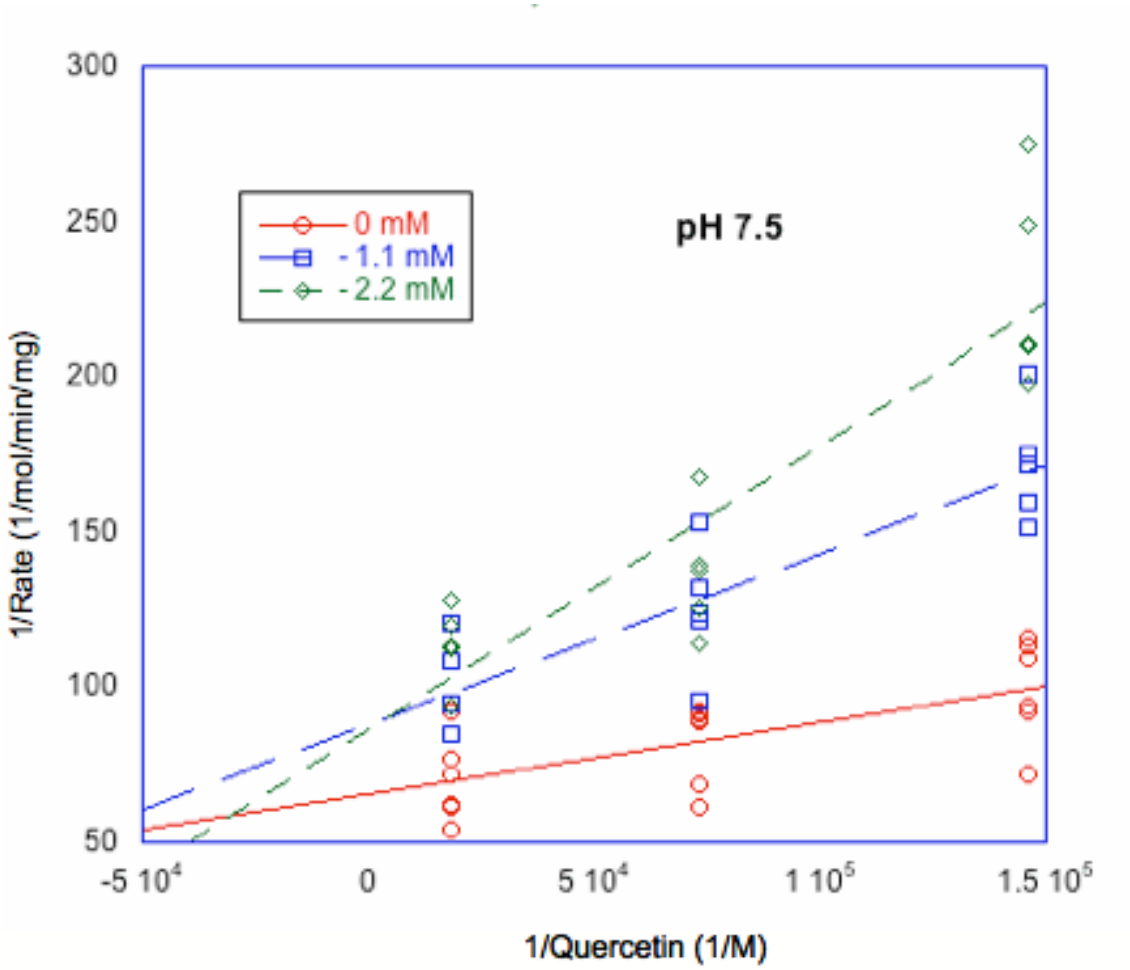

FIG. 4.6: **The inhibition of BsQueD by 373p was observed at pH 7.5**. The 1.1 mM and 2.2 mM inhibitor lines intersect at the y-axis, but they appear to intersect the 0 mM inhibitor line beyond the y-axis.

TABLE. 4.2

Kinetic parameters of the inhibiton of BsQueD by 373p at pH 7.5.

	V_{max} (mol/min/mg)	K_m (M)
0 mM 373p	$1.58x10^{-2}±1.22x10^{-3}$	$3.59x10^{-6}±1.36x10^{-6}$
1.1 mM 373p	$1.13x10^{-2}±7.81x10^{-4}$	$5.83x10^{-6}±1.52x10^{-6}$
2.2 mM 373p	$1.03x10^{-2}±7.48x10^{-4}$	7.33x10-6±$1.80x10^{-6}$
K_i (M)	$4.82x10^{-5}$	

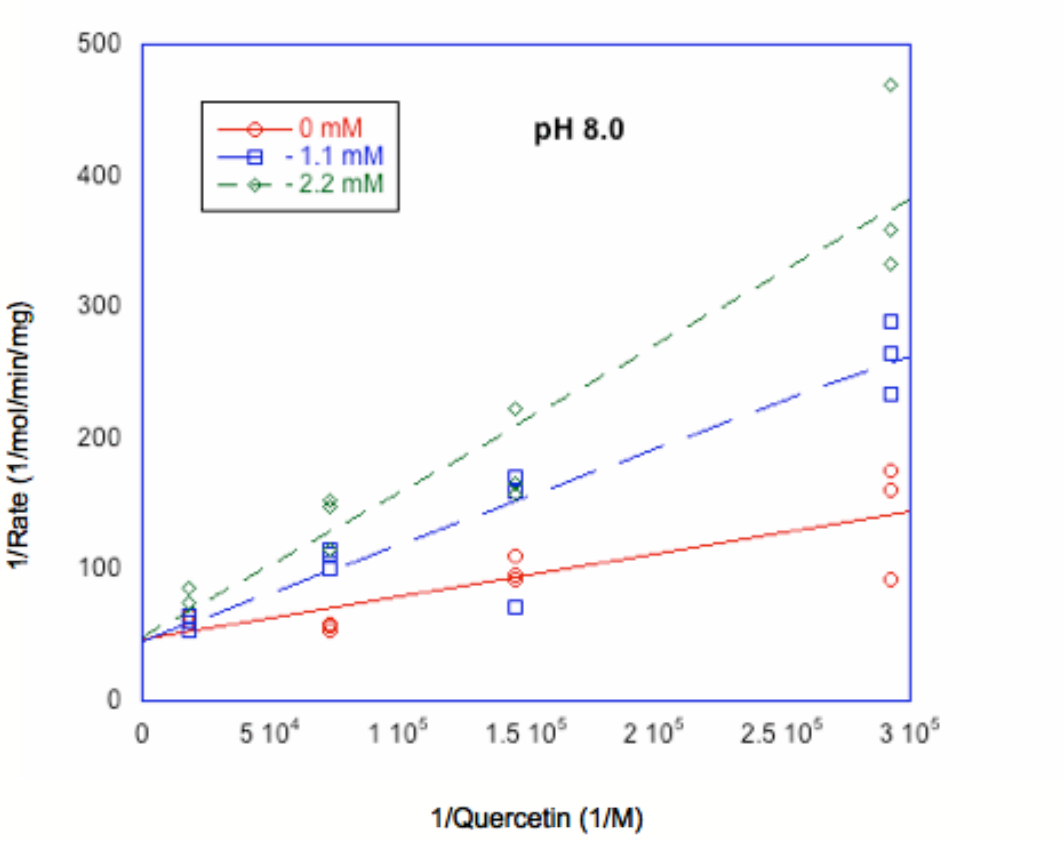

FIG.4.7: **The inhibition of BsQueD by 373p appears to be competitive at pH 8.0.**

TABLE. 4.3

Kinetic parameters of the inhibition of BsQueD by 373p at pH 8.0.

	V_{max} (mol/min/mg)	K_m (M)
0 mM 373p	$1.87x10^{-2}\pm1.85x10^{-3}$	$4.29x10^{-6}\pm1.53x10^{-6}$
1.1 mM 373p	$2.04x10^{-2}\pm2.79x10^{-3}$	$1.29x10^{-5}\pm4.52x10^{-6}$
2.2 mM 373p	$1.63x10^{-2}\pm1.16x10^{-3}$	$1.54x10^{-5}\pm2.69x10^{-6}$
K_i (M)	$1.74x10^{-5}$	

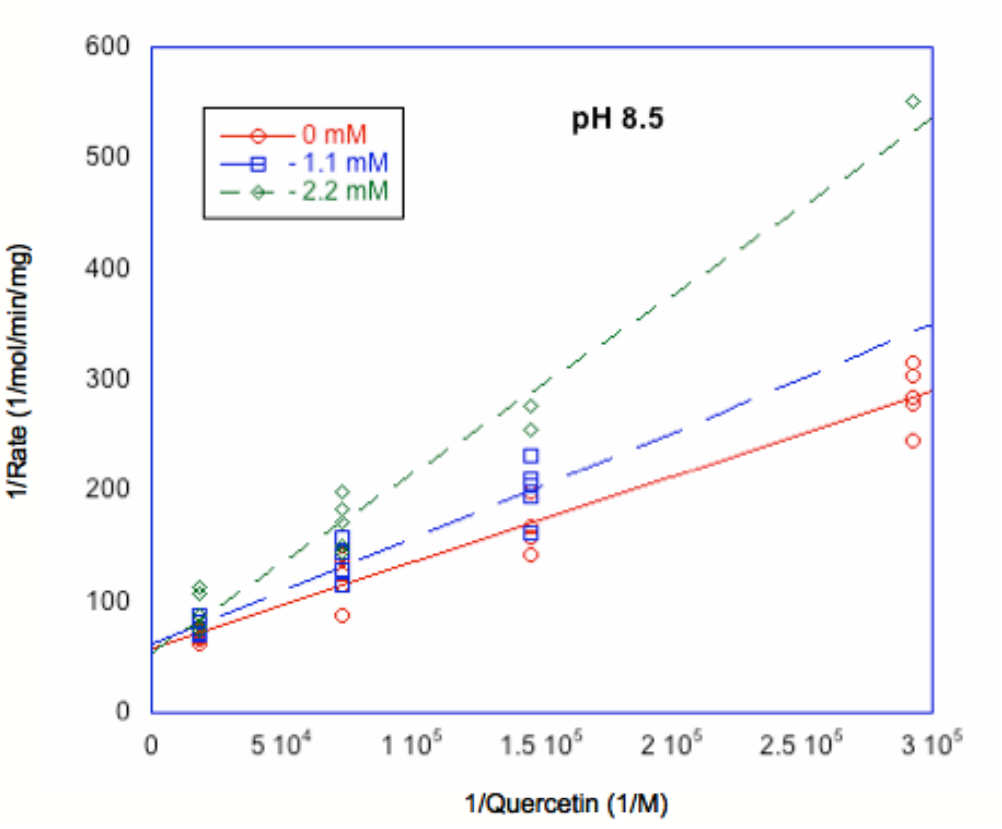

FIG. 4.8: **The inhibition of BsQueD by 373p at pH 8.5 seems to be competitive**. But the reaction is likely more complicated.

TABLE 4.4

Kinetic parameters of the inhibition of BsQueD by 373p at pH 8.5.

	V_{max} (mol/min/mg)	K_m (M)
0 mM 373p	$1.86x10^{-2}$±$1.02x10^{-3}$	$1.52x10^{-5}$±$2.05x10^{-6}$
1.1 mM 373p	$1.70x10^{-2}$±$1.00x10^{-3}$	$1.72x10^{-5}$±$2.55x10^{-6}$
2.2 mM 373p	$1.58x10^{-2}$±$1.89x10^{-3}$	$2.26x10^{-5}$±$6.56x10^{-6}$
K_i (M)	$1.69x10^{-4}$	

TABLE. 4.5

A comparison of the K_i values of the inhibition of BsQueD by 373p at various pH.

pH	K_i
7.5	$4.82x10^{-5}$ M
8.0	$1.74x10^{-5}$M
8.5	$1.69x10^{-4}$M

Another possible inhibitor of BsQueD has been found and tested briefly. 3,7-dihydroxyflavone ((37DHF) FIG. 4.5) seems to behave as a competitive inhibition in the catalytic reaction of BsQueD (FIG. 4.9).

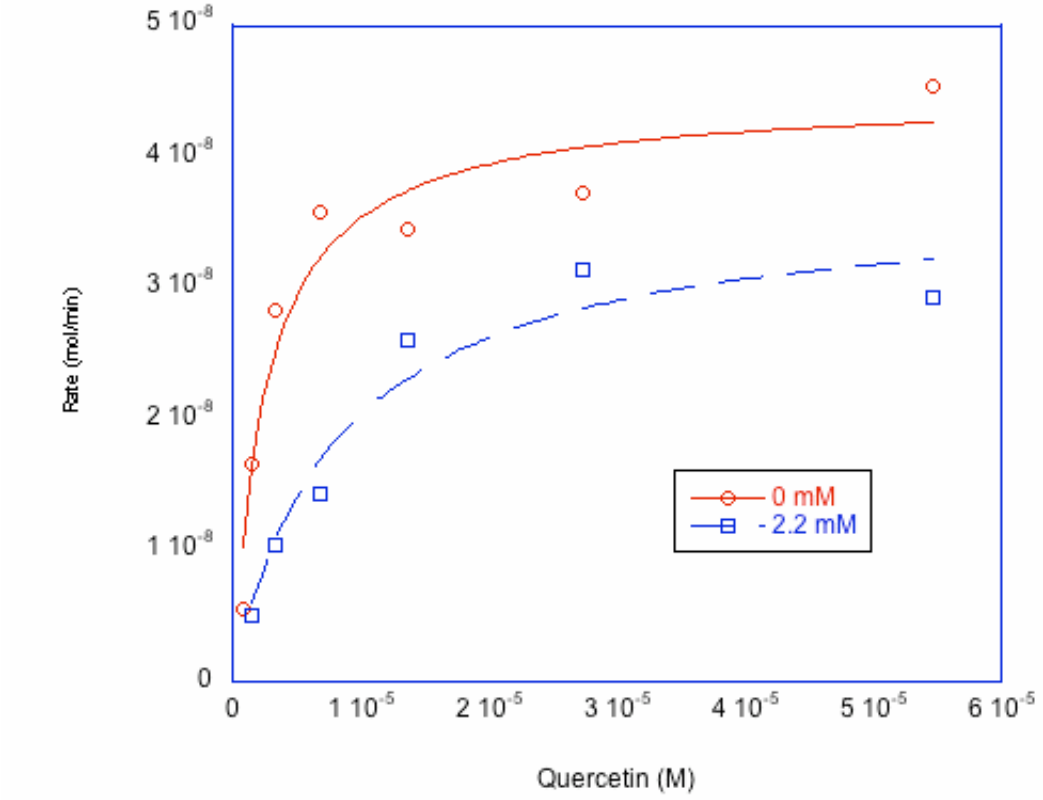

FIG. 4.9: **37DHF seems to behave as a competitive inhibitor**. Future analysis must be done.

TABLE. 4.6

The preliminary kinetic parameters of the inhibition of BsQueD by 37DHF

	V_{max} (mol/min)	K_m (M)
0 mM 37DHF	$4.46\text{x}10^{-8}\pm1.89\text{x}10^{-9}$	$2.63\text{x}10^{-6}\pm4.49\text{x}10^{-7}$
2.2 mM 37DHF	$4.37\text{x}10^{-8}\pm7.40\text{x}10^{-9}$	$2.85\text{x}10^{-5}\pm1.02\text{x}10^{-5}$
K_i (M)	$5.56\text{x}10^{-6}$	

DISCUSSION

The optimal storage conditions for BsQueD were found by preparing several samples of BsQueD under different salt, glycerol and temperature conditions and testing their retention of activity over a period of several weeks. It is very clear that BsQueD remains more active when stored at -20˚C rather than at 4˚C. Any detriment that three freeze/thaw cycles might have had on the enzyme were far less damaging than keeping them at 4˚C. All the frozen samples retained at least 49% activity, and seven of the eight samples retained greater than 70% activity. This was not the case for the 4˚ samples, however. Only the 20% glycerol samples stored at 4˚ C were at 70% or greater activity after eighteen days. Samples containing 20% glycerol retained the most activity regardless of storage temperature. Glycerol has long been known to stabilize proteins, but it is still not entirely clear why this molecule has such an effect. The most plausible explanation is that the dipole-dipole interaction of glycerol interacts with the aqueous solvent (51).

Kojic acid's inhibitory effect has already been shown with another quercetinase from the genus *Aspergillus* (52). This example of quercetin (AQueD), discussed in chapters 1 and 2, contains one atom of Cu(II) as opposed to two atoms of Mn(II). In fact a crystal structure of AQueD complexed with KA has been solved (53), and it appears that KA binds with the Cu(II) in the

active site of the enzyme. Interestingly, preliminary studies of the inhibition of KA have been conducted with BsQueD (54). In these studies the enzyme was incubated with KA and then enzyme activity was compared to that of control (enzyme without KA), and it was found that BsQueD retained 100% of its activity. This seems inconsistent with the results of the latest experiments. It is possible that the concentrations of substrate tested were not high enough to obtain a true maximum velocity, but this cannot explain the consistent K_m values obtained. More trials with higher substrate concentrations and more concentrations of KA should be conducted to fully understand this system.

The inhibition of BsQueD by 37DHF and 373p both appear to be competitive at several pH conditions, but the reactions are more complicated than originally expected, and therefore, a more in-depth analysis must be completed.

REFERENCES

51. Arakawa, T. and Timasheff, S. N. (1985) Theory of Protein Solubility *Methods in Enzymology* 114, 49-77.

52. Bentley, R. (2006) From miso, sake and shoyu to cosmetics: a century of science for kojic acid *Natural Product Reports*, 23 1046-1062.

53. Steiner, R. A., Kooter, I. M., and Dijkstra, B. W. (2002) Functional analysis of the copper-dependent quercetin 2,3-dioxygenase. 1. Ligand-induced coordination changes probed by X-ray crystallography: Inhibition, ordering effect, and mechanistic insights. *Biochemistry 41*, 7955-7962.

54. Schaab, M. R., Barney, B. M., and Francisco, W. A. (2006) Kinetic and spectroscopic studies on the quercetin 2,3-dioxygenase from Bacillus subtilis. *Biochemistry 45*, 1009-1016.

REFERENCES

1. Voet, D., Voet, J. G., and Pratt, C. W. (2002) *Fundamentals of Biochemistry Upgrade Ed.* John Wiley & Sons, Inc, United States of America

2. Dunwell, J. M., Purvis, A., and Khuri, S. (2004) Cupins: the most functionally diverse protein superfamily? *Phytochemistry 65*, 7-17.

3. Dunwell, J. M., Culham, A., Carter, C. E., Sosa-Aguirre, C. R., and Goodenough, P. W. (2001) Evolution of functional diversity in the cupin superfamily. *Trends in Biochemical Sciences 26*, 740-746.

4. Dai, Y., Pochapsky, T. C., and Abeles, R. H. (2001) Mechanistic studies of two dioxygenases in the methionine salvage pathway of *Klebsiella pneumoniae*. *Biochemistry 40*, 6379-6387.

5. Dai, Y., Wensink, P. C., and Abeles, R. H. (1999) One protein, two enzymes. *Journal of Biological Chemistry 274*, 1193-1195.

6. Hawkins, A. R., and Lamb, H. K. (1995) The molecular biology of multidomain proteins - selected examples. *European Journal of Biochemistry 232*, 7-18.

7. Bugg, T. D. H. (2001) Oxygenases: mechanisms and structural motifs for O-2 activation. *Current Opinion in Chemical Biology 5*, 550-555.

8. Bugg, T. D. H. (2003) Dioxygenase enzymes: catalytic mechanisms and chemical models. *Tetrahedron 59*, 7075-7101.

9. Klinman, J. P. (2001) Life as aerobes: are there simple rules for activation of dioxygen by enzymes? *Journal of Biological Inorganic Chemistry 6*, 1-13.

10. Klinman, J. P. (2007) How Do Enzymes Activate Oxygen without Inactivating Themselves? *Accounts of Chemical Research* 40, 325-333.

11. Oka, T., Simpson, F. J., Child, J. J., and Mills, C. (1971) Degradation of rutin by *Aspergillus flavus* - Purification of

dioxygenase, quercetinase. *Canadian Journal of Microbiology 17*, 111-&.

12. Steiner, R. A., Kalk, K. H., and Dijkstra, B. W. (2002) Anaerobic enzyme-substrate structures provide insight into the reaction mechanism of the copper-dependent quercetin 2,3-dioxygenase. *Proceedings of the National Academy of Sciences of the United States of America 99*, 16625-16630.
13. Steiner, R. A., Kooter, I. M., and Dijkstra, B. W. (2002) Functional analysis of the copper-dependent quercetin 2,3-dioxygenase. 1. Ligand-induced coordination changes probed by X-ray crystallography: Inhibition, ordering effect, and mechanistic insights. *Biochemistry 41*, 7955-7962.

14. Fusetti, F., Schroter, K. H., Steiner, R. A., van Noort, P. I., Pijning, T., Rozeboom, H. J., Kalk, K. H., Egmond, M. R., and Dijkstra, B. W. (2002) Crystal structure of the copper-containing quercetin 2,3-dioxygenase from *Aspergillus japonicus*. *Structure 10*, 259-268.

15. Barney, B. M., Schaab, M. R., LoBrutto, R., and Francisco, W. A. (2004) Evidence for a new metal in a known active site: purification and characterization of an iron-containing quercetin 2,3-dioxygenase from *Bacillus subtilis*. *Protein Expression and Purification 35*, 131-141.

16. Bowater, L., Fairhurst, S. A., Just, V. J., and Bornemann, S. (2004) *Bacillus subtilis* YxaG is a novel Fe-containing quercetin 2,3-dioxygenase. *Febs Letters 557*, 45-48.

17. Schaab, M. R., Barney, B. M., and Francisco, W. A. (2006) Kinetic and spectroscopic studies on the quercetin 2,3-dioxygenase from Bacillus subtilis. *Biochemistry 45*, 1009-1016.

18. Nidetzky, G. D. S. a. B. (2006) Variations of the 2-His-1-carboxylate Theme in Mononuclear non-Heme FeII Oxygenases. *ChemBioChem 7*, 1536-1548.

19. Gabbianelli, R., Battistoni, A., Polizio, F., Carri, M. T., Demartino, A., Meier, B., Desideri, A., and Rotilio, G. (1995) Metal uptake of recombinant cambialistic superoxide dismutase from *Propionibacterium shermanii* affected by growth conditions of

host *Escherichia coli* cells. *Biochemical and Biophysical Research Communications 216*, 841-847.

20. Gopal, B., Madan, L. L., Betz, S. F., and Kossiakoff, A. A. (2005) The crystal structure of a quercetin 2,3-dioxygenase from *Bacillus subtilis* suggests modulation of enzyme activity by a change in the metal ion at the active site(s). *Biochemistry 44*, 193-201.

21. Schaab, M. R. (2006).

22. Gopal, B., Madan, L. L., Betz, S. F., and Kossiakoff, A. A. (2005) The crystal structure of a quercetin 2,3-dioxygenase from *Bacillus subtilis* suggests modulation of enzyme activity by a change in the metal ion at the active site(s). *Biochemistry 44*, 193-201.

23. Steiner, R. A., Kalk, K. H., and Dijkstra, B. W. (2002) Anaerobic enzyme-substrate structures provide insight into the reaction mechanism of the copper-dependent quercetin 2,3-dioxygenase. *Proceedings of the National Academy of Sciences of the United States of America 99*, 16625-16630.

24. Schaab, M. R., Barney, B. M., and Francisco, W. A. (2006) Kinetic and spectroscopic studies on the quercetin 2,3-dioxygenase from Bacillus subtilis. *Biochemistry 45*, 1009-1016.

25. Dunwell, J. M., Purvis, A., and Khuri, S. (2004) Cupins: the most functionally diverse protein superfamily? *Phytochemistry 65*, 7-17.

26. Fusetti, F., Schroter, K. H., Steiner, R. A., van Noort, P. I., Pijning, T., Rozeboom, H. J., Kalk, K. H., Egmond, M. R., and Dijkstra, B. W. (2002) Crystal structure of the copper-containing quercetin 2,3-dioxygenase from *Aspergillus japonicus*. *Structure 10*, 259-268.

27. Catic, A., Sun, Z. J., Ratner, D. M., Misaghi, S., Spooner, E., Samuelson, J., Wagner, G. and Ploegh, H. L. (2007) Sequence and structure evolved separately in ribosomal ubiquitin variant. *EMBO Journal* 26, 3474-3483.

28. Ho, S. N., Hung, H. D., Horton, R. M., Pullen, J. K., and Pease, L. R. (1989) Site-directed mutagenesis by overlap extension using the polymerase chain reaction. *Gene* 77, 51-59.

29. Notredame, C., Higgins, D. G., and Heringa, J. (2000) T-Coffee: A Novel Method for Fast and Accurate Multiple Sequence Alignment. *Journal of Molecular Biology* 302, 205-217.

30. UCSF Chimera--a visualization system for exploratory research and analysis. Pettersen EF, Goddard TD, Huang CC, Couch GS, Greenblatt DM, Meng EC, Ferrin TE. *J Comput Chem.* 2004 Oct;25(13):1605-12.

31. Esposito, D. and Chatterjee, D. K. (2006) Enhancement of soluble protein expression through the use of fusion tags. *Biotechnology* 17, 353-358.

32. Woestenenk, E. A., Hammarstrom, M., van den Berg, S., Hard, T., and Berglund, H. (2004) His tag effect on solubility of human proteins produced in *Escherichia coli*: a comparison between four expression vectors. *Journal of Structural and Functional Genomics* 5, 217-229.

33. Moomaw, E. W., Angerhofer, A., Moussatche, P., Ozarowski, A., Garcia-Rubio, I. and Richards, N. G. J. (2009) Metal Dependence of Oxalate Decarboxylase Activity. *Biochemistry* 48, 6116-6125.

34. Merkins, H., Kappl, R., Jokob, R. P., Schmid, F. X., and Fetzner, S. (2008) Quercetinase QueD of Streptomyces sp. FLA, a monocupin Dioxygenase with a Preference for Nickel and Cobalt. *Biochemistry* 47, 12185-12196.

35. Balogh-Hergovich, E. and Speier G. (2001) Kinetics and Mechanism of the Base-Catalyzed Oxygenation of Flavonol in DMSO-H_2O Solution. *Journal of Oragnic Chemistry* 66, 7974-7978.

36. Hoffman, B. J., Broadwater, J. A., Johnson, P., Harper, J., Fox, B. G., and Kenealy, W. R. (1995) Lactose fed-batch overexpression of recombinant metalloproteins in Excherichia coli BL21-(DE3)-

process control yielding high levels of metal incorporated, soluble protein. *Protein Expression Purification* 6, 646-654.

37. Tottey, S., Waldron, K. J., Firbank, S. J., Reale, B., Bessant, C., Sato, K., Cheek, T. R., Gray, J., Banfield, M. J., Dennison, C., and Robinson, N. (2008) Protein-folding location can regulate manganese-binding versus copper- or zinc-binding. *Nature* 455, 1138-1142.

38. Oka, T., Simpson, F. J., Child, J. J., Mills, S. C. (1971) Degradation of rutin by Aspergillus flavus. Purification of the dioxygenase, quercetinase. *Canadian Journal of Microbiology* 17, 111-118.

39. Svedruzic, D., Liu, Y., Reinhardt, L. A., Wroclawska, E., Cleland, W. C., and Richards, N. G. J. (2007) Investigating the roles of putative active site residues in the oxalate decarboxylase from *Bacillus subtilis*. *Archives of Biochemistry and Biophysics* 464, 36-47.

40. Garret, R. H., and Grisham, C. M. (2005) *Biochemistry 3rd Ed.* Brooks/Cole, Belmont, p 112.

41. Voet, D., Voet, J. G., and Pratt, C. W. (2002) *Fundamentals of Biochemistry Upgrade Ed.* John Wiley & Sons, Inc, United States of America, pp 96-99.

42. Matthews, C. K., van Holde, K. E., and Ahern, K. G. (2000) *Biochemistry 3rd Ed.* Addison Wesley Longman, San Francisco, p 148.

43. Barney, B. M., Schaab, M. R., LoBrutto, R., and Francisco, W. A. (2004) Evidence for a new metal in a known active site: purification and characterization of an iron-containing quercetin 2,3-dioxygenase from *Bacillus subtilis*. *Protein Expression and Purification 35*, 131-141.

44. Gasteiger E, Hoogland C, Gattiker A, Duvaud S, Wilkins M R, Appel R D, Bairoch A, *Protein Identification and Analysis Tools on the ExPASy Server*, (In) *John M. Walker (ed): The Proteomics Protocols Handook* (2005) Humana Press, pp 571-607. http://www.expasy.org/tools/aldente/

45. Ho, S. N., Hung, H. D., Horton, R. M., Pullen, J. K., and Pease, L. R. (1989) Site-directed mutagenesis by overlap extension using the polymerase chain reaction. *Gene* 77, 51-59.

46. Greenfield, N. J. (2007) Using circular dichroism spectra to estimate protein secondary structure. *Nature Protocols* 1, 2876-2890.

47. Kabsch W., Sander C. (1983) Dictionary of protein secondary structure: pattern recognition of hydrogen-bonded and geometrical features. *Biopolymers*

48. Esposito, D. and Chatterjee, D. K. (2006) Enhancement of soluble protein expression through the use of fusion tags. *Biotechnology* 17, 353-358.

49. Woestenenk, E. A., Hammarstrom, M., van den Berg, S., Hard, T., and Berglund, H. (2004) His tag effect on solubility of human proteins produced in *Escherichia coli*: a comparison between four expression vectors. *Journal of Structural and Functional Genomics* 5, 217-229.

50. Gopal, B., Madan, L. L., Betz, S. F., and Kossiakoff, A. A. (2005) The crystal structure of a quercetin 2,3-dioxygenase from *Bacillus subtilis* suggests modulation of enzyme activity by a change in the metal ion at the active site(s).

51. Arakawa, T. and Timasheff, S. N. (1985) Theory of Protein Solubility *Methods in Enzymology* 114, 49-77.

52. Bentley, R. (2006) From miso, sake and shoyu to cosmetics: a century of science for kojic acid *Natural Product Reports*, 23 1046-1062.

53. Steiner, R. A., Kooter, I. M., and Dijkstra, B. W. (2002) Functional analysis of the copper-dependent quercetin 2,3-dioxygenase. 1. Ligand-induced coordination changes probed by X-ray crystallography: Inhibition, ordering effect, and mechanistic insights. *Biochemistry 41*, 7955-7962.

54. Schaab, M. R., Barney, B. M., and Francisco, W. A. (2006) Kinetic and spectroscopic studies on the quercetin 2,3-dioxygenase from Bacillus subtilis. *Biochemistry 45*, 1009-1016.

This document was generated using the Graduate College Format Advising tool. Please turn a copy of this page in when you submit your document to Graduate College format advising. You may discard this page once you have printed your final document. DO NOT TURN THIS PAGE IN WITH YOUR FINAL DOCUMENT!

121

121

121